AUTOPHAGY
2022, VOL. 18, NO. 12, 2781–2798
https://doi.org/10.1080/15548627.2022.2047384

Taylor & Francis
Taylor & Francis Group

RESEARCH PAPER

OPEN ACCESS Check for updates

TRAF6 autophagic degradation by *avibirnavirus* VP3 inhibits antiviral innate immunity via blocking NFKB/NF-κB activation

Tingjuan Deng[a], Boli Hu[a], Xingbo Wang[a], Shuxiang Ding, Lulu Lin[a], Yan Yan[a], Xiran Peng[a], Xiaojuan Zheng[a], Min Liao[a], Yulan Jin[a], Weiren Dong[a], Jinyan Gu[a], and Jiyong Zhou[a,b]

[a]MOA Key Laboratory of Animal Virology, Center for Veterinary Sciences, Zhejiang University, Hangzhou, Zhejiang Province, China; [b]Collaborative innovation center and State Key Laboratory for Diagnosis and Treatment of Infectious Diseases, First Affiliated Hospital, Zhejiang University, Hangzhou, Zhejiang Province, China

ABSTRACT

Ubiquitination is an important reversible post-translational modification. Many viruses hijack the host ubiquitin system to enhance self-replication. In the present study, we found that *Avibirnavirus* VP3 protein was ubiquitinated during infection and supported virus replication by ubiquitination. Mass spectrometry and mutation analysis showed that VP3 was ubiquitinated at residues K73, K135, K158, K193, and K219. Virus rescue showed that ubiquitination at sites K73, K193, and K219 on VP3 could enhance the replication abilities of infectious bursal disease virus (IBDV), and that K135 was essential for virus survival. Binding of the zinc finger domain of TRAF6 (TNF receptor associated factor 6) to VP3 mediated K11- and K33-linked ubiquitination of VP3, which promoted its nuclear accumulation to facilitate virus replication. Additionally, VP3 could inhibit TRAF6-mediated NFKB/NF-κB (nuclear factor kappa B) activation and IFNB/IFN-β (interferon beta) production to evade host innate immunity by inducing TRAF6 autophagic degradation in an SQSTM1/p62 (sequestosome 1)-dependent manner. Our findings demonstrated a macroautophagic/autophagic mechanism by which *Avibirnavirus* protein VP3 blocked NFKB-mediated IFNB production by targeting TRAF6 during virus infection, and provided a potential drug target for virus infection control.

Abbreviations: ATG: autophagy related; BafA1: bafilomycin A_1; CALCOCO2/NDP52: calcium binding and coiled-coil domain 2; Cas9: CRISPR-associated protein 9; CHX: cycloheximide; Co-IP: co-immunoprecipitation; CRISPR: clustered regularly interspaced short palindromic repeats; GAPDH: glyceraldehyde-3-phosphate dehydrogenase; GST: glutathione S-transferase; IBDV: infectious bursal disease virus; IF: indirect immunofluorescence; IFNB/IFN-β: interferon beta; mAb: monoclonal antibody; MAP1LC3/LC3: microtubule associated protein 1 light chain 3; MOI: multiplicity of infection; MS: mass spectrometry; NFKB/NF-κB: nuclear factor kappa B; NBR1: NBR1 autophagy cargo receptor; OPTN: optineurin; pAb: polyclonal antibody; PRRs: pattern recognition receptors; RNF125: ring finger protein 125; RNF135/Riplet: ring finger protein 135; SQSTM1/p62: sequestosome 1; TAX1BP1: tax1 binding protein1; TCID50: 50% tissue culture infective dose; TRAF3: TNF receptor associated factor 3; TRAF6: TNF receptor associated factor 6; TRIM25: tripartite motif containing 25; Ub: ubiquitin; Wort: wortmannin; WT: wild type.

ARTICLE HISTORY
Received 27 August 2021
Revised 21 February 2022
Accepted 24 February 2022

KEYWORDS
*Avibirnavirus*VP3 ubiquitination; innate antiviral immune; nuclear trafficking; selective autophagy; SQSTM1; TRAF6 degradation

Introduction

Ubiquitination, a reversible post-translational modification, participates in multiple biological processes, including substrate protein stability, subcellular transport, and signaling transduction [1–5]. Ubiquitin (Ub) is conjugated to lysine (K) residues of substrate proteins by an enzymatic cascade, including E1 activation enzymes, E2 conjugation enzymes, and E3 ubiquitin ligases [6,7]. Ub contains seven lysine residues K6, K11, K27, K29, K33, K48, and K63 and gives rise to multiple potential polyubiquitin signals [8]. Importantly, the type of polyubiquitination determines the different biological effects. K11-, K33-, and K63-linked polyubiquitination have been shown to be relevant to signaling transduction, protein stability, trafficking, and subcellular distribution [4,5,9–13], whereas, K48-linked polyubiquitination is commonly involved in ubiquitin-proteasome degradation [14]. Recently, many studies have reported that ubiquitination participates in the life cycle of diverse viruses, e.g., *Avibinavirus* [15], influenza A virus [16–19], porcine circovirus type 2 [20], Ebola virus [21], and *Senecavirus A* [22] .

Infectious bursal disease virus (IBDV), the representative member of the genus *Avibirnavirus*, belongs to the *Birnaviridae* family [23]. The genome of IBDV is a double-strand RNA (dsRNA) comprising segment A and segment B [24]. Segment A encodes nonstructural protein VP5 and structural proteins VP2, VP3, and VP4 [25,26]. Segment B encodes the RNA-dependent RNA polymerase VP1 [27,28]. Many reports demonstrated that IBDV protein VP3 plays an important role in virus morphogenesis, the negative regulation of type I interferon (IFN) β, and cell autophagy [29–31]. The impact of VP3 ubiquitination on viral replication are

CONTACT Jiyong Zhou jyzhou@zju.edu.cn MOA Key Laboratory of Animal Virology, Zhejiang University, 866 Yuhangtang Road, Hangzhou 310058, Zhejiang Province, P. R. China

Supplemental data for this article can be accessed here

unclear, although the roles of chemical modification of VP1 and VP4 have been reported [15,25,32,33].

An increasing number of E3 ubiquitin ligases are implicated to resist virus infection by mediating host antiviral immune responses [34]. However, many viruses have evolved elaborate mechanisms to hijack host E3 ubiquitin ligases to support self-replication [21,35–39]. TRAF6 (TNF receptor associated factor 6), an E3 ubiquitin ligase, plays an essential role in the NFKB/NF-κB (nuclear factor kappa B) signaling pathway and multiple pattern recognition receptor (PRR) signaling pathways [40]. In the NFKB signaling pathway, TRAF6 is auto-ubiquitinated through K63-linked ubiquitin chains [41], followed by activation of a complex comprising MAP3K7/TAK1 (mitogen-activated protein kinase kinase kinase 7), TAB2 (TGF-beta activated kinase 1 [MAP3K7] binding protein 2), and TAB3 (TGF-beta activated kinase 1 (MAP3K7) binding protein 3) [42–44]. This complex then induces phosphorylation of the IKK (inhibitor of IKBKB/IκB kinase) complex (CHUK/IKKα, IKBKB/IKKβ, and IKBKG/IKKγ), resulting in activation of NFKB and IFNB/IFN-β production [45]. In addition, TRAF6's E3 ubiquitin ligase activity can also mediate host protein ubiquitination, and affects substrate protein stability and subcellular localization [3,4,10]. However, to the best of our knowledge, TRAF6-mediated viral protein ubiquitination has not been reported.

The objective of this study was to explore whether *Avibirnavirus* protein VP3 undergoes ubiquitination and, if so, how this might regulate its function. We demonstrated that VP3 was a ubiquitinated protein during infection and interacts with the zinc finger domain of TRAF6 to promote its ubiquitination, which facilitated VP3 nuclear accumulation and virus replication. Surprisingly, we found that VP3 induced TRAF6 autophagic degradation in an SQSTM1/p62 (sequestosome 1)-dependent manner, which inhibited TRAF6-dependent NFKB activation and IFNB production to support viral replication.

Results

Avibirnavirus VP3 protein undergoes ubiquitination during infection

To detect the chemical modification of *Avibirnavirus* VP3 protein, lysates from IBDV-infected DF-1 or 293 T cells were subjected to immunoblotting assays. The results showed that VP3, with an approximate molecular mass of 40–100 kDa, was detected (Figure 1A), which displayed a similar modified phenotype in avian DF-1 cells and human 293 T cells. To confirm that the protein bands with larger molecular weights were the ubiquitinated VP3, the lysates of IBDV-infected DF-1 cells and 293 T cells co-transfected with *MYC-VP3* (VP3 overexpression) and *HA-Ub* (Ubiquitin overexpression) plasmids were subjected to immunoprecipitation with anti-VP3 or anti-MYC mouse monoclonal antibodies (mAbs), respectively. The results showed that VP3 was heavily modified by polyubiquitin chains (Figure 1B and 1C). However, ubiquitinated VP3 was not detected in purified IBDV particles (Figure 1D), suggesting that ubiquitination of VP3 was strictly controlled during the different stages of the viral life cycle. Taken together, these data suggested that VP3 was ubiquitinated during infection.

Avibirnavirus VP3 has multiple ubiquitination sites

To identify the ubiquitination sites on *Avibirnavirus* VP3, mass spectrometry (MS) assays were used. The results showed that VP3 contained five ubiquitination sites: K73, K135, K158, K193, and K219 (Figure 2A). To further verify these ubiquitination sites, we constructed different mutants of VP3 bearing single Lys (K)-to-Arg (R) substitutions and all five substitutions (5KR) and performed immunoprecipitation assays. The results revealed that polyubiquitin chain conjugation to the K73R, K135R, K158R, K193R, and K219R mutants were reduced in comparison with wild-type (WT) VP3 (Figure 2B) and the ubiquitination of 5KR mutant VP3 was almost completely abolished (Figure 2C), confirming that residues K73, K135, K158, K193 and K219 were the major ubiquitination sites on VP3.

VP3 directly binds to TRAF6 to block proteasome degradation and enhance nuclear localization

Ubiquitination affects protein stability [22,46]. To investigate the impact of ubiquitin on VP3 stability, 293 T cells were co-transfected with vectors expressing MYC-VP3 or MYC-VP3 ubiquitination site mutants along with HA-Ub, and then subjected to immunoblotting and reverse transcription PCR (RT-PCR) assays. The results showed that ubiquitin strongly increased the protein level of WT VP3, but not that of the VP3[5KR] mutant, although the levels of both WT and 5KR mutant *VP3* mRNA did not change significantly (Figure 3A). Meanwhile, Ubiquitin (Ub) overexpression markedly increased the half-life of VP3 in cells treated with cycloheximide (CHX) to block *de novo* protein synthesis (Figure 3B). These findings demonstrated that ubiquitination of VP3 contributed to protein stability rather than degradation.

Ubiquitin E3 ligases are necessary for the ubiquitin system [47]. To determine the E3 ubiquitin ligase that modulated VP3, several host E3 ubiquitin ligases, TRAF3 (TNF receptor associated factor 3), TRAF6, RNF125 (ring finger protein 125), RNF135 (ring finger protein 135), TRIM25 (tripartite motif containing 25), and TAX1BP1 (Tax1 binding protein1), were selected. Among the selected E3 ligases, western blotting detected that only TRAF6 overexpression obviously enhanced VP3 protein stability (**Fig. S1**), indicating that TRAF6 was relevant to the stability of VP3. Subsequently, the interaction between TRAF6 and VP3 was detected. As shown in Figure 3C and 3D, co-immunoprecipitation (co-IP) assays showed that TRAF6 interacted with VP3 during co-transfection or IBDV infection. In addition, *in vitro* glutathione-S-transferase (GST) affinity-isolation assays further confirmed the direct association between TRAF6 and VP3 (Figure 3E). To determine whether TRAF6 served as an E3 ligase for VP3 ubiquitination, we detected the level of polyubiquitin linkages on VP3 in the presence or absence of TRAF6. As shown in Figures 3F and 3G, the level of VP3 ubiquitination was dramatically enhanced by TRAF6 overexpression. Considering that the type of polyubiquitin chains

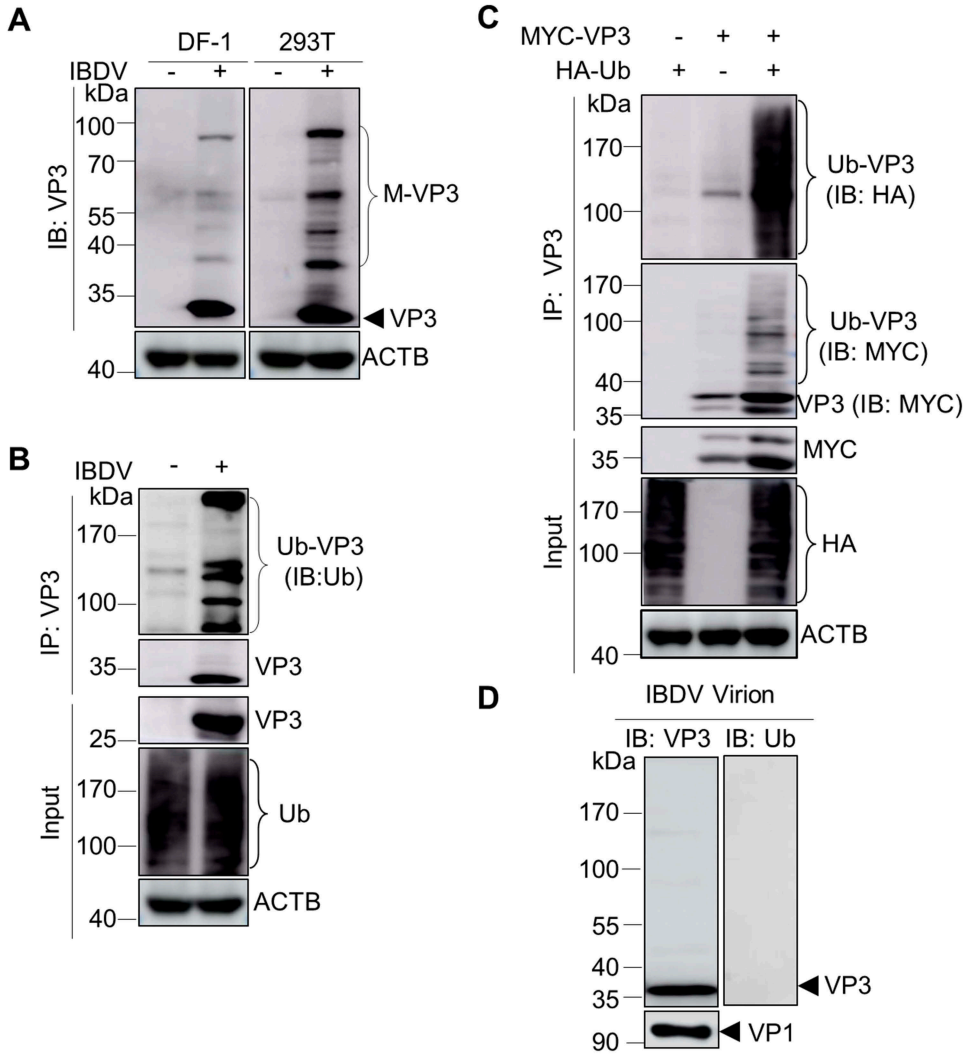

Figure 1. *Avibirnavirus* VP3 is ubiquitinated during infection. (**A**) Western blotting analysis of viral protein VP3. DF-1 and 293 T cells were infected with IBDV (MOI = 10) for 12 h. Cellular lysates were subjected to western blotting with anti-VP3 mouse mAbs. (**B**) Viral protein VP3 undergoes ubiquitination during infection. IBDV-infected DF-1 cells at an MOI of 10. At 12 h after infection, cellular lysates were used for VP3-immunoprecipitation and western blotting with anti-ubiquitin and anti-VP3 mouse mAbs. (**C**) VP3 is ubiquitinated during transfection. 293 T cells were co-transfected with vectors expressing MYC-VP3 and HA-Ub for 48 h. Cellular lysates were subjected to an immunoprecipitation assay with anti-VP3 mouse mAbs and western blotting with the indicated antibodies. (**D**) Ubiquitinated VP3 is not present in purified IBDV particles. IBDV virions were subjected to western blotting analysis using anti-ubiquitin and anti-VP3 mouse mAbs.

conjugated to the lysine residues of the substrate protein provokes distinct biological effects [48–51], we detected ubiquitin linkage types conjugated onto VP3 driven by TRAF6. The results showed that TRAF6 was the major E3 ubiquitin ligase that catalyzes K11- and K33-linked polyubiquitination of VP3 (Figure 3H). Subsequently, we assessed if Lys 73, 135, 158, 193, and 219 in VP3 were the major sites of TRAF6-mediated ubiquitination. As shown in Figure 3I, ubiquitin chains conjugation to the VP3 Lys 73, 135, 158, 193, and 219 Arg mutants was greatly reduced in TRAF6 expressing cells compared with those of WT VP3, and the promotion of TRAF6 on VP3 ubiquitination was almost completely abolished when the five lysines were substituted with arginine. Taken together, these data demonstrated that TRAF6 enhanced the K11- and K33-linked ubiquitination of VP3 at Lys 73, 135, 158, 193, and 219.

To investigate if TRAF6-mediated ubiquitination played a role in modulating the stability of VP3, we evaluated the levels of WT and 5KR mutant VP3 protein in 293 T cells overexpressing TRAF6. As shown in Figure 3J, overexpression of Ub and TRAF6 greatly enhanced the WT VP3 protein level, but not the level of VP3[5KR], and the level of *VP3* mRNA showed no obvious change. However, TRAF6 still could upregulate the levels of the K73R, K135R, K158R, K193R, and K219R mutants dramatically **(Fig. S2)**. These results demonstrated that TRAF6 might increase the stability of VP3 through inducing its ubiquitination. To further assessed the impact of TRAF6 on VP3 stability, cells expressing MYC-VP3 or co-expressing MYC-VP3 and FLAG-TRAF6 (TRAF6 overexpression) were treated with CHX or the ubiquitin proteasome inhibitor, MG132. We observed that VP3 levels were gradually reduced in CHX treated cells without FLAG-TRAF6 overexpression, but overexpressing TRAF6 prevented such reduction (Figure 3K). Meanwhile, VP3 gradually accumulated upon MG132 treatment in cells with or without TRAF6 overexpression, and was higher in

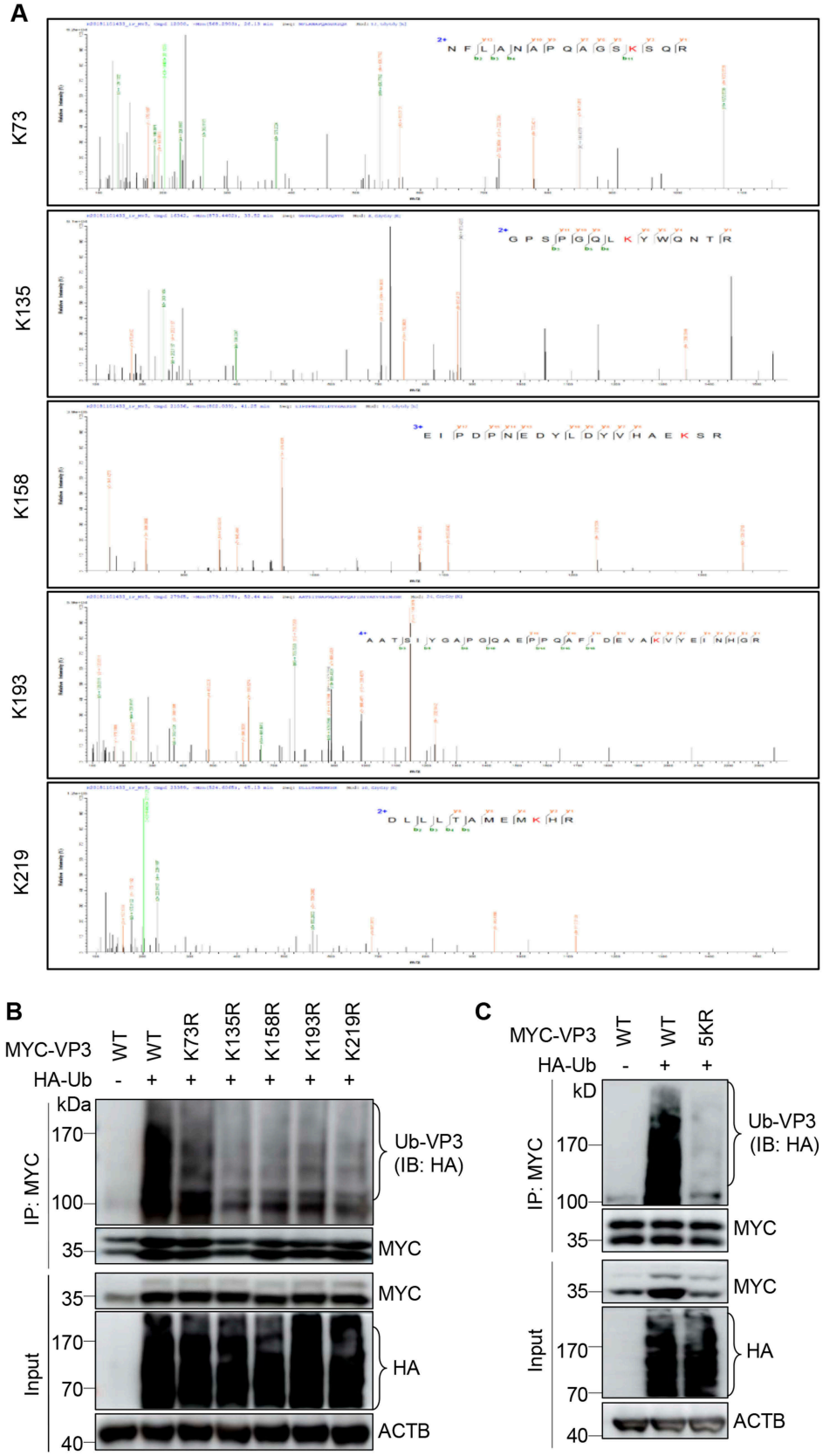

Figure 2. Identification of ubiquitination sites on VP3. (**A**) Mass spectrometry identification of ubiquitinated VP3 revealed multiple ubiquitination sites. (**B** and **C**) Confirmation of the ubiquitination sites on VP3 using an immunoprecipitation assay. Vectors expressing MYC-VP3 and its mutants, together with HA-Ub, were separately co-transfected into 293 T cells for 48 h. The lysates were subjected to VP3-immunoprecipitation and western blotting with the indicated antibodies.

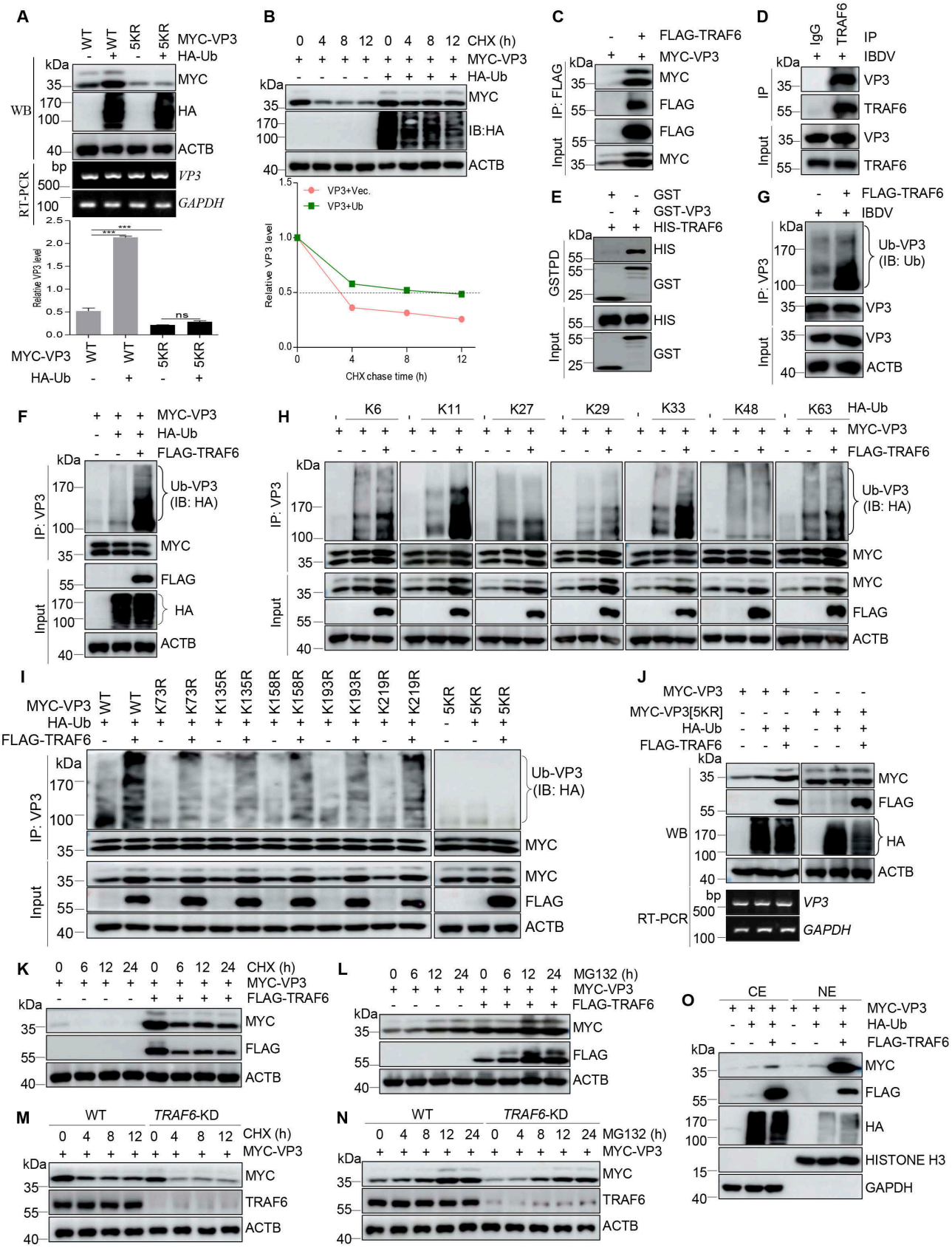

Figure 3. Viral protein VP3 targeting to TRAF6 enhances its stability via blocking proteasome-mediated degradation. (**A**) Ubiquitin overexpression increases the stability of the WT VP3 protein but not the 5KR mutant VP3. 293 T cells were co-transfected with vectors expressing MYC-VP3 or MYC-VP3[5KR] and HA-Ub for 24 h. Western blotting and RT-PCR assays were used separately to assess the expression levels of VP3 protein and mRNA. (**B**) Ubiquitin prolongs the lifespan of viral protein VP3. Vectors expressing MYC-VP3 and HA-Ub or empty vector were co-transfected into 293 T cells for 24 h, followed by treatment with CHX (100 μg/ml). (**C** and **D**) TRAF6 interaction with viral protein VP3. Cellular lysates from 293 T cells transfected with vectors expressing FLAG-TRAF6 and MYC-VP3 (C) or DF-1 cells infected with IBDV (D) were subjected to co-IP and western blotting assays using the indicated antibodies. (**E**) TRAF6 interaction with viral protein VP3 by GST affinity-isolation

TRAF6-overexpressed cells (Figure 3L). Consistently, in *TRAF6* deficient 293 T cells constructed using the clustered regularly interspaced short palindromic repeats-Cas9 (CRISPR-Cas9) method **(Fig. S3)**, as shown in Figures 3M **and** 3N, VP3 had shorter life span and lower accumulation in *TRAF6* deficient 293 T cells treated with CHX and MG132, respectively.

In addition, TRAF6-mediated ubiquitination was reported to promote the nuclear trafficking of substrates to enhance protein stability [4,10]. Thus, to determine if TRAF6-mediated ubiquitination of VP3 involves modulation of VP3 nuclear transport, VP3 was analyzed by an immunoblotting assay in the cytoplasm and nucleus of 293 T cells co-transfected with *MYC-VP3, HA-Ub*, and *FLAG-TRAF6*. As shown in Figure 3O, the accumulation of VP3 increased significantly in the nuclear fraction of cells overexpressing TRAF6. These findings indicated that VP3 directly bound to TRAF6 to enhance its nuclear accumulation by blocking proteasome-dependent degradation of VP3.

The zinc finger domain of TRAF6 is crucial to enhance the stability and nuclear accumulation of viral protein VP3

To explore if the increase of VP3 stability induced by TRAF6 depended on the RING domain with E3 ubiquitin ligase activity, we constructed a TRAF6 mutant possessing a cysteine (C)-70-to-alanine (A) substitution in the RING domain and found that overexpression of WT, and the C70A mutant TRAF6, greatly enhanced the concentration of VP3 (Figure 4A), suggesting that TRAF6-mediated VP3 stability was RING domain-independent. Thus, we hypothesized that TRAF6 involved in the stability of VP3 functions through other domains. Subsequently, we constructed different TRAF6-truncation mutants, named as TRAF6ΔRING, TRAF6ΔZN, TRAF6ΔZinc and TRAF6ΔTRAF-C mutants (Figure 4B), and detected their interaction with VP3. In western blotting and co-IP assays, we observed that WT TRAF6, TRAF6ΔRING and TRAF6ΔTRAF-C, but not TRAF6ΔZN and TRAF6-ΔZinc, interacted with VP3 and increased its stability (Figure 4C). To eliminate the impact of high expression, we only assessed the association of TRAF6ΔZN or TRAF6ΔZinc and VP3, and discovered that the zinc finger domain deletion of TRAF6 abolished the interaction with VP3 (Figure 4D).

Similarly, to investigate whether the ubiquitination sites on VP3 affected the binding to TRAF6, the interaction of different VP3 mutants with TRAF6 were detected using co-IP and western blotting. The results exhibited that 5KR mutant VP3 completely lost the ability to interact with TRAF6 and the interaction of VP3 ^{K135R} mutant with TRAF6 also was reduced significantly. However, the TRAF6 association with VP3 mutants K73R, K158R, K193R or K219R hardly changed compared with that of WT VP3 (Figures 4E **and** 4F). Subsequently, we further revealed that the zinc finger domain was essential for TRAF6-mediated VP3 ubiquitination (Figure 4G). Notably, a recent study revealed that zinc region might have E3 ubiquitin ligase activity [52]. Thus, we speculated that TRAF6-mediated ubiquitination of VP3 might be zinc finger domain-dependent rather than RING domain. Subsequently, to investigate whether the mutant TRAF6^{C70A} retained a capacity to mediate VP3 ubiquitination, we constructed different E2 conjugation enzymes and determined that UBE2D1 (ubiquitin conjugating enzyme E2 D1) was co-binding partner of TRAF6 and viral protein VP3 **(Fig. S4A and S4B)**. Moreover, by *in vitro* ubiquitination assay, we verified that the VP3 ubiquitination driven by TRAF6-UBE2D1 complex was irrelevant to RING domain activity of TRAF6 (Figure 4H). Additionally, we observed that TRAF6-mediated VP3 nuclear accumulation also depended on its zinc finger domain (Figure 4I). Altogether, these data demonstrated that VP3 interacted with the zinc finger domain on TRAF6, which was crucial to enhance the stability and nuclear accumulation of VP3.

The zinc finger domain of TRAF6 mediates VP3 ubiquitination and is crucial for sustaining virus replication

To evaluate the impact of ubiquitination of VP3 at K73, K135, K158, K193, or K219 on IBDV replication, T7 RNA polymerase promoter rescue plasmid, *T7-A*, possessing VP3^{K73R}, VP3^{K135R}, VP3^{K158R}, VP3^{K193R}, VP3^{K219R}, or VP3[5KR] were generated by mutation using the wild type *T7-A* plasmid as the template. These mutants and wild-type *T7-A* along with *T7-B* were separately co-transfected into BSRT7 cells, followed by infection of fresh DF-1 cells. As shown in Figure 5A, except for the recombinant mutants rK135R and r5KR, the recombinant viruses rWT, rK73R, rK158R, rK193R, and rK219R successfully rescued IBDV replication, indicating

assay. (**F** and **G**) TRAF6 promotes VP3 ubiquitination. The lysates from 293 T cells overexpressing MYC-VP3 and FLAG-TRAF6 along with HA-Ub were immunoprecipitated with anti-VP3 mAbs and immunoblotted using the indicated antibodies (F). 293 T cells transfected with vectors expressing FLAG-TRAF6 for 24 h were infected with IBDV for 12 h, and then an immunoprecipitation assay was performed with anti-VP3 mouse mAbs (G). (**H**) TRAF6 mainly mediates K11- and K33-linked ubiquitination of VP3. Vectors expressing MYC-VP3 and FLAG-TRAF6 together with HA-Ub mutants (K6, K11, K27, K29, K33, K48, and K63) were co-transfected separately into 293 T cells for 48 h. The lysates were immunoprecipitated with anti-VP3 mAbs and immunoblotted using the indicated antibodies. (**I**) TRAF6 catalyzes ubiquitination of VP3 at Lys 73, 135, 158, 193 and 219. 293 T cells were co-transfected with vectors expressing MYC-VP3 or its mutants, HA-Ub, and FLAG-TRAF6 for 48 h. Then cellular lysates were immunoprecipitated and subjected to immunoblotting assays as described in (H). (**J**) TRAF6 increases the stability of VP3. Cellular lysates from 293 T cells transfected with vectors expressing MYC-VP3 or mutant MYC-VP3[5KR], HA-Ub, and FLAG-TRAF6 were subjected to immunoblotting and RT-PCR assays. (**K** and **L**) TRAF6 overexpression suppresses proteasome-dependent degradation of VP3. 293 T cells were co-transfected with vectors expressing MYC-VP3 and FLAG-TRAF6 or empty vector for 24 h, followed by treatment with CHX (100 mg/ml) (K) or MG132 (10 μM) (L) for the indicated times. (**M** and **N**) TRAF6 knockdown promotes proteasome-mediated degradation of VP3. WT and TRAF6 incompletely knockout 293 T cells were transfected with vectors expressing MYC-VP3 for 24 h, respectively. Cells were then treated with CHX (M) and MG132 (N) as described in (K and L). Cellular lysate samples from (B), (H) and (K-L) were subjected to western blotting with the indicated antibodies. (**O**) TRAF6 markedly promotes the nuclear accumulation of VP3. 293 T cells transfected with vectors expressing MYC-VP3 together with HA-Ub, FLAG-TRAF6 or HA-Ub and FLAG-TRAF6 were harvested and then subjected to cellular fractionation, as described in the Materials and Methods. Finally, the levels of VP3 in cytoplasmic elements (CEs) and nuclear elements (NEs) were analyzed by immunoblotting using the indicated antibodies. GAPDH and HISTONE H3 served as markers of CE and NE, respectively.

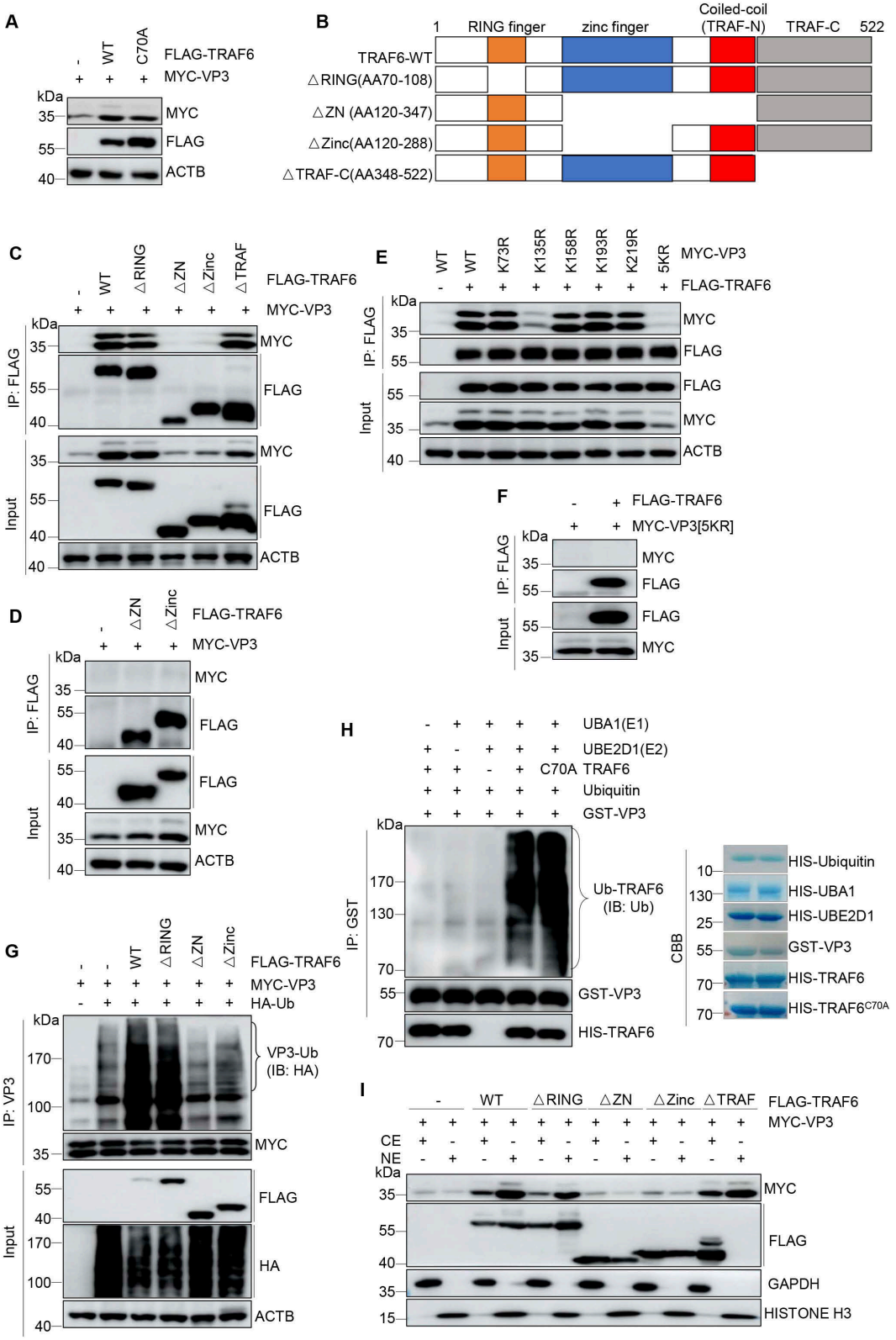

Figure 4. Viral protein VP3 binding to the zinc finger domain of TRAF6 mediated its ubiquitination. (**A**) The RING domain of TRAF6 with E3 ubiquitin activity had no impact on VP3 stability. 293 T cells were co-transfected with vectors expressing WT or C70A mutant TRAF6 and MYC-VP3 for 24 h. Cellular lysates were subjected western blotting assays with the indicated antibodies. (**B**) Schematic representation of TRAF6 and its truncated mutants. (**C** and **D**) The zinc finger domain of TRAF6 was required for the interaction with VP3. *MYC-VP3* and *FLAG-TRAF6* or *TRAF6* deletion mutants were co-transfected into 293 T cells. Cellular lysates were subjected to FLAG-immunoprecipitation and western blotting using the indicated antibodies. (**E** and **F**) Ubiquitination sites on VP3 were required for binding to TRAF6. 293 T cells were co-transfected with vectors expressing MYC-VP3 or VP3 mutants and FLAG-TRAF6 for 48 h. Cellular lysates were subjected to immunoprecipitation with anti-FLAG mouse mAbs and western blotting assays using the indicated antibodies. (**G**) The zinc finger domain of TRAF6-mediated ubiquitination of VP3. Cellular lysates from 293 T cells overexpressing MYC-VP3, HA-Ub, and FLAG-TRAF6 or TRAF6 deletion mutants were subjected to an immunoprecipitation assay with anti-VP3 mouse mAbs and a western blotting assay using the indicated antibodies. (**H**) *In vitro* ubiquitination assays showed that the RING domain activity was unnecessary for TRAF6-mediated ubiquitination of VP3. IPTG-inducible HIS-tagged recombinant proteins E1(UBA1), UBE2D1, ubiquitin, TRAF6, TRAF6^{C70A} and GST-VP3 were expressed

that the ubiquitination of VP3 at K135 was essential for virus survival. Subsequently, $TCID_{50}$ detection exhibited that *in vitro* the replication abilities of the viruses rK73R, rK193R, and rK219R were markedly decreased in comparison with the rWT virus, and that the rK158R mutation was insignificant (Figure 5B). The consistent data was also obtained in the rK158R virus but not rK73R, rK193R virus infected bursal tissues of the specific pathogen free (SPF) chickens by RT-qPCR assay (Figure 5C). However, the histopathological analysis showed that rK158R and rK193R recombinant viruses, but not rK73R and rK219R viruses, induced more obvious lesions in the bursae of SPF chickens in comparison with rWT, rK73R and rK219R (Figure 5D), suggesting that the substitution of K158R and K193R in VP3 could strengthen the pathogenicity of IBDV. Collectively, these data demonstrated that the ubiquitination of VP3 supported viral replication.

Given that the zinc finger domain of TRAF6 was critical for VP3 binding and mediating its ubiquitination, we investigated the impact of overexpression or knockdown of TRAF6 on IBDV replication by detecting virus replication. $TCID_{50}$ detection showed that the virus titer increased significantly in TRAF6 overexpressing DF-1 cells infected with IBDV and decreased significantly in cells expressing a short hairpin RNA (shRNA) targeting *TRAF6* compared with that in control cells infected with IBDV (Figure 5E-**G**). Meanwhile, we observed that WT TRAF6, but not TRAF6ΔZinc, dramatically promoted IBDV replication (Figure 5H). Considering that chicken is the natural host of IBDV infection, we further investigated the relationship of chicken TRAF6 and viral protein VP3. The results showed that chicken TRAF6 associated with VP3 and enhanced VP3 stability and IBDV proliferation by its zinc finger domain (**Fig. S5A-D**). Collectively, these results indicated that the ubiquitination sites of VP3 binding to the zinc finger domain of TRAF6 was necessary to ensure IBDV replication.

VP3 facilitates TRAF6 autophagic degradation

Considering that TRAF6 interacted with VP3, and IBDV infection induced an increase of LC3B expression and a decrease of TRAF6 and SQSTM1 expression *in vitro* and *in vivo* (Figure 6A), we hypothesized that VP3 might participate TRAF6 degradation in autophagosome-dependent manner. Therefore, we conducted a western blotting experiment for VP3 and TRAF6. The results revealed that VP3 significantly decreased the level of TRAF6 in a dose-dependent manner (Figure 6B). However, there was no significant change in the level of the *TRAF6* transcript (Figure 6C), which suggested that VP3 affected the stability of TRAF6. Next, we assessed the impact of VP3 on the half-life of TRAF6 using CHX treatment. The results demonstrated that the half-life of exogenous TRAF6 was significantly shortened in WT and 5KR mutant VP3 overexpressing cells compared with that of the control (Figures 6D **and** 6E). However, in comparison with WT VP3, TRAF6 was quickly degraded in the VP3[5KR] mutant overexpressing cells (Figure 6E). Moreover, the loss of ubiquitination at any ubiquitin sites of VP3 accelerated the degradation of TRAF6 by VP3 (**Fig. S6**).

Autophagy and the ubiquitin-proteasome system are two major intracellular degradative pathways. To determine if VP3 facilitated TRAF6 degradation by autophagy, an experiment using autophagy inhibitors, wortmannin (Wort) and bafilomycin A_1 (BafA1) was conducted. As shown in Figure 6F, VP3-mediated TRAF6 degradation was almost blocked using the autophagy inhibitors Wort and BafA1, but not by MG132. To further confirm the role of autophagosomes in VP3-induced TRAF6 degradation, we constructed autophagy-related genes *ATG7* and *ATG5* knockout 293 T cells (**Fig. S7A and S7B**). *ATG7* knockout almost completely blocked VP3-induced TRAF6 degradation (Figure 6G), whereas *ATG5* knockout partially inhibited TRAF6 degradation induced by VP3 (Figure 6H). Collectively, our data indicated that VP3-mediated degradation of TRAF6 was an autophagosome-dependent event.

VP3 blocks NFKB activation by promoting autophagic degradation of TRAF6 in SQSTM1/p62-dependent manner

To identify the proteins responsible for the autophagic degradation of TRAF6, we investigated the role of autophagy receptors, such as SQSTM1, OPTN (optineurin), CALCOCO2/NDP52 (calcium binding and coiled-coil domain 2), NBR1(NBR1 autophagy cargo receptor) and TAX1BP1 [53]. Of the five receptors, only SQSTM1 interacted with TRAF6 and strongly promoted TRAF6 degradation (**Fig. S8A and S8B**). To further identify the domain of SQSTM1 responsible for mediating the degradation of TRAF6, we constructed a series of SQSTM1-truncation mutants, deleting the ubiquitin-binding domain (UBA) responsible for binding to ubiquitinated substrates [54], Phox1 and Bem1p (PB1) required for activating autophagy [55], TRAF-binding domain (TBS), and the LC3-interacting region (LIR) that is critical for recruiting substrates into autophagosomes for lysosomal degradation [56]. The PB1, TBS, and LIR-deleted SQSTM1 mutants obviously decreased TRAF6 degradation in comparison with WT SQSTM1 and the UBA-deleted SQSTM1 mutant (**Fig. S8C**), suggesting that SQSTM1 mediated TRAF6 autophagic degradation.

To further detect whether VP3-induced autophagic degradation of TRAF6 was SQSTM1-dependent, we analyzed the relationship between SQSTM1 and VP3. Co-IP assays showed that VP3 only interacted significantly with SQSTM1 (Figures 7A **and** 7B). Subsequently, *SQSTM1*-deficient 293 T cells were generated (Figure 7C), and western blotting demonstrated that VP3-induced TRAF6 degradation was

in *E. coli* BL21 and purified as described in materials and methods. These purified proteins were identified by Coomassie Brilliant Blue staining (right) and used for *in vitro* ubiquitination assays. Finally, the samples were analyzed by western blotting using indicated antibodies (left). (**I**) The zinc finger domain on TRAF6 was necessary for the nuclear accumulation of VP3. Vectors expressing MYC-VP3 and FLAG-TRAF6 or TRAF6 deletion mutants were co-transfected into 293 T cells for 24 h. The cellular lysates were subjected to cellular fractionation as described in the Materials and methods, and western blotting assays were used for the detection of VP3 in the CE and NE. GAPDH and HISTONE H3 served as markers of the CE and NE, respectively.

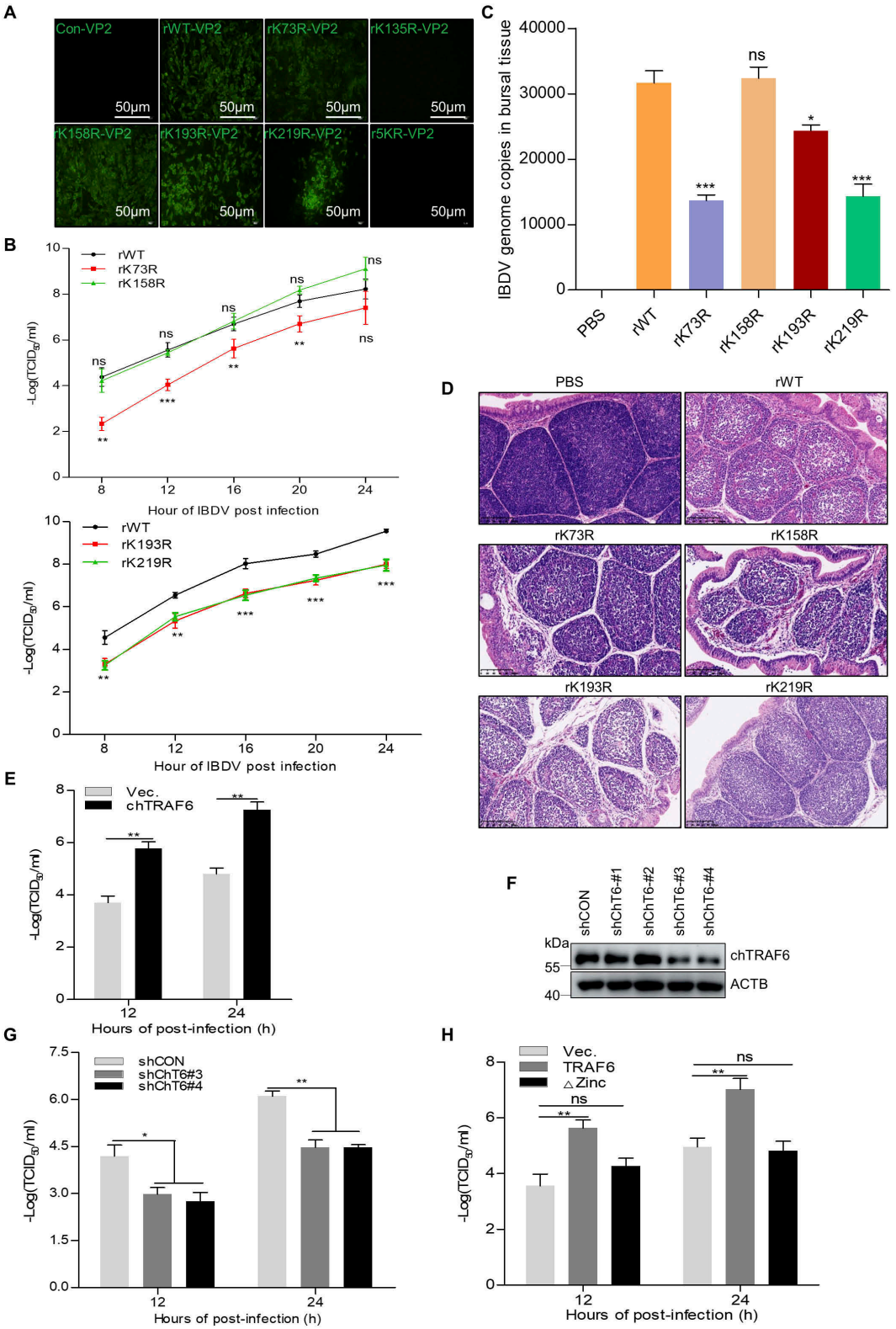

Figure 5. The zinc finger domain of TRAF6 binding to VP3 is essential to support viral replication. (**A**) IFA analysis of recombinant viruses. DF-1 cells were infected with recombinant rWT or mutant virus for 18 h, followed by IFA assay with antibodies against viral protein VP2, as described in the Materials and methods. (**B**) The one step growth curve of rescued viruses. DF-1 cells were infected with recombinant viruses rWT, rK73R, rK158R, rK193R, and K219R, respectively. At the indicated time after infection, cells were harvested and subjected to virus titer detection by the $TCID_{50}$. (**C**) Copies of IBDV genome were detected by RT-qPCR *in vivo*. ns: $p > 0.05$ nonsignificant difference, $^{*}p < 0.05$, $^{***}p < 0.001$ significant difference. (**D**) Histopathological examination of bursae at 5 dpi. (**E**) chTRAF6 overexpression facilitates IBDV replication. DF-1 cells transfected with vectors expressing FLAG-chTRAF6 or the corresponding empty vector were infected with IBDV (MOI = 10) for the indicated times. Cellular lysates were used for virus titer detection. (**F**) Screening of an efficient shRNA against ch*TRAF6*. Four shRNA against *TRAF6* were cloned into vector pGreenPuro™ shRNA (Biovector Science Lab, Inc., SI505A-1). These constructs and a control (scramble) shRNA were transfected separately into DF-1 cells for 48 h. Cellular lysates were subjected to western blotting using anti-chTRAF6 antibody. ACTB levels served as the loading control. Oligonucleotide sequences for an shRNA against chicken *TRAF6* are listed in Table S3. (**G**) ChTRAF6 knockdown suppresses IBDV replication. The two effective shchT6#3 and shchT6#4 and a negative control shCON were transfected into DF-1 cells for 24 h, respectively. The resultant cells were infected, and then the viral titers were detected as described in (B). (**H**) The zinc finger domain of TRAF6 interacting with VP3 is necessary to promote virus replication. DF-1 cells overexpressing WT or zinc finger domain deletion mutant TRAF6 were infected with IBDV (MOI = 10). At 12 and 24 h after infection, cells were harvested and subjected to virus titer detection according to the $TCID_{50}$.

dramatically blocked in *SQSTM1* knockout cells (Figures 7D **and** 7E), indicating that VP3-induced TRAF6 degradation was SQSTM1-dependent. To further analyze whether IBDV VP3 protein could drive receptor SQSTM1-mediated selective autophagy, we detected impacts of VP3 overexpression on the autophagy level in cells with or without SQSTM1. As shown in Figure 7F, the capacity of VP3 on the induction of autophagy was almost completely abolished in *SQSTM1*-deficient cells, which indicated that VP3 could facilitate selective autophagy via SQSTM1. In addition, given that TRAF6 interaction with SQSTM1 increased selective autophagy [57], we hypothesized that the association of TRAF6 and SQSTM1 could be elevated by IBDV or viral protein VP3. As shown in Figures 7G **and** 7H, the interaction between TRAF6 and SQSTM1 was significantly enhanced in the presence of IBDV, WT VP3, or VP3[5KR] mutants. In addition, we observed that WT VP3 and VP3[5KR] obviously accelerated SQSTM1-induced TRAF6 degradation (Figure 7I). These findings clearly indicated that IBDV VP3 facilitated selective autophagy degradation of TRAF6 through increasing the association of TRAF6 with SQSTM1.

PRR recognition of double-stranded RNA leads to the recruitment of TRAF6, which then drives NFKB activation and IFNB production [40]. Additionally, viral protein VP3 binding to dsRNA can efficiently inhibit type I interferon β production [30]. Therefore, we assessed whether SQSTM1 participated in VP3-induced inhibition of NFKB-mediated IFNB induction. We observed that the levels of phosphorylated CHUK/IKKα-IKBKB/IKKβ and RELA/p65 were notably inhibited in VP3 overexpressed cells stimulated with poly I:C, but this inhibition was abolished in *SQSTM1* knockout cells (Figure 7J), indicating that the inhibition of VP3 on NFKB activation was SQSTM1-dependent event. Subsequently, we detected the effects of VP3 on TRAF6-driven *NFKB* and *IFNB* promoter activation in WT and *SQSTM1* knockout cells. The results revealed that the VP3-induced negative regulation of type I IFN activation was abolished in *SQSTM1* knockout cells (Figures 7K **and** 7L). Taken together, our data indicated that VP3 targeted to the cargo receptor SQSTM1 mediated TRAF6 autophagic degradation, which led to the inhibition of NFKB-mediated antiviral signaling.

Discussion

The host ubiquitin (Ub) system plays important roles against diverse virus infections. TRIM22 and TRIM32 induce K48-linked polyubiquitination of the nucleocapsid protein (NP) and polymerase basic protein 1 (PB1) of influenza A virus for degradation and to restrict viral replication, respectively [16,49]. The pRNF114 protein mediates K27-linked polyubiquitination of the NS4B protein of swine fever virus, leading to its degradation [51]. However, recently, many studies have revealed that Ub system can be hijacked by viruses to promote viral proliferation. E3 ligase ASB8 and E2 ubiquitin-conjugating enzyme UBE2L6 separately promote the ubiquitination of the Nsp1α protein of porcine reproductive and respiratory syndrome virus and RNA polymerase 3D of *Senecavirus* A to enhance stability and facilitate virus replication [22,50]. In the present study, our data demonstrated that the stability of *Avibirnavirus* VP3 could be enhanced via ubiquitination, leading to the promotion of viral replication (Fig. 3A, 3B, 5B **and** 5C). Additionally, we also revealed that ubiquitinated VP3 could be detected in IBDV-infected cells, but not in purified virions, which indicated that ubiquitination of VP3 was strictly controlled during infection and did not participate in the assembly of IBDV virions. Similarly, NP and PB1 proteins of influenza A virus can be efficiently conjugated to ubiquitin during replication and these ubiquitinated proteins are not incorporated into mature viral particles [16,49].

In this study, viral protein VP3 exhibited the K11- and K33-linked polyubiquitination by interacting directly with zinc finger domain of TRAF6, which increased VP3 nuclear accumulation (Fig. 3H **and** 4G **and** I). E3 ubiquitin ligases mediate the transfer of ubiquitin from an E2 ubiquitin-conjugating enzyme to specific substrate proteins [47]. To mediate self-ubiquitination and regulate viral replication, host E3 ubiquitin ligases can be employed by viral proteins, e.g., Ebola virus protein VP35 [21], porcine circovirus type 2 Cap protein [20], the polymerase basic protein 1 and nucleocapsid protein of influenza A virus [16,17,49,58], and the Nsp1α protein of porcine reproductive and respiratnory syndrome virus [50]. Previous studies demonstrated that TRAF6-mediated polyubiquitination modulates the subcellular trafficking of the substrate protein to enhance its stability [2,10]. Moreover, the RING and zinc finger domains on TRAF6 are essential for its ubiquitin E3 ligase activity [59]. Thereby, we concluded that during *Avibirnavirus* replication, VP3 hijacks TRAF6 for supporting viral proliferation. Additionally, our recent study reveals that *Avibirnavirus* VP3 in nucleus can target directly and de-SUMOylate API5 to repress IFNB production [60], implying that TRAF6-mediated VP3 ubiquitination enhanced its nuclear accumulation to inhibit API5-mediated IFN expression (Figure 8).

TRAF6 is also an important adaptor of NFKB and diverse PRR pathways [40,61]. The activation of NFKB regulates the production of type I IFNs [62]. Many viruses can evade host antiviral response through affecting the expression or activity of TRAF6, such as human immunodeficiency virus-1 [63], human parainfluenza virus type 2 [64], human T-cell leukemia virus type 1 [3], and classical swine fever virus [65]. Additionally, IFNB plays a critical role in the host response against IBDV infection [66]. Moreover, *Avibirnavirus* protein VP3 is inhibitor of IFIH1/MDA5-induced IFNB production [30]. In present study, IBDV infection or VP3 overexpression induced decreased TRAF6 levels, and VP3 promoted the autophagic degradation of TRAF6 by targeting autophagic receptor SQSTM1, finally resulting in the inhibition of NFKB activation-dependent IFNB production induced by TRAF6. Thus, we believe that *Avibirnavirus* protein VP3 inactivated TRAF6-dependent antiviral innate immunity to support viral replication.

Notably, *Avibirnavirus*-encoded VP4 had been identified as a serine protease and a phosphoprotein, which contributes the cleavage of viral polyprotein precursor (NH2-pVP2-VP4-VP3 -COOH) [25,67,68]. In recent years, increasing evidences shows that some viral proteinases, i.e. aichi virus 3C protease [69], coxsackievirus B3 (CVB3) viral proteinase 2A [70] and Seneca Valley virus (SVV) $3C^{pro}$ [71], can target selective

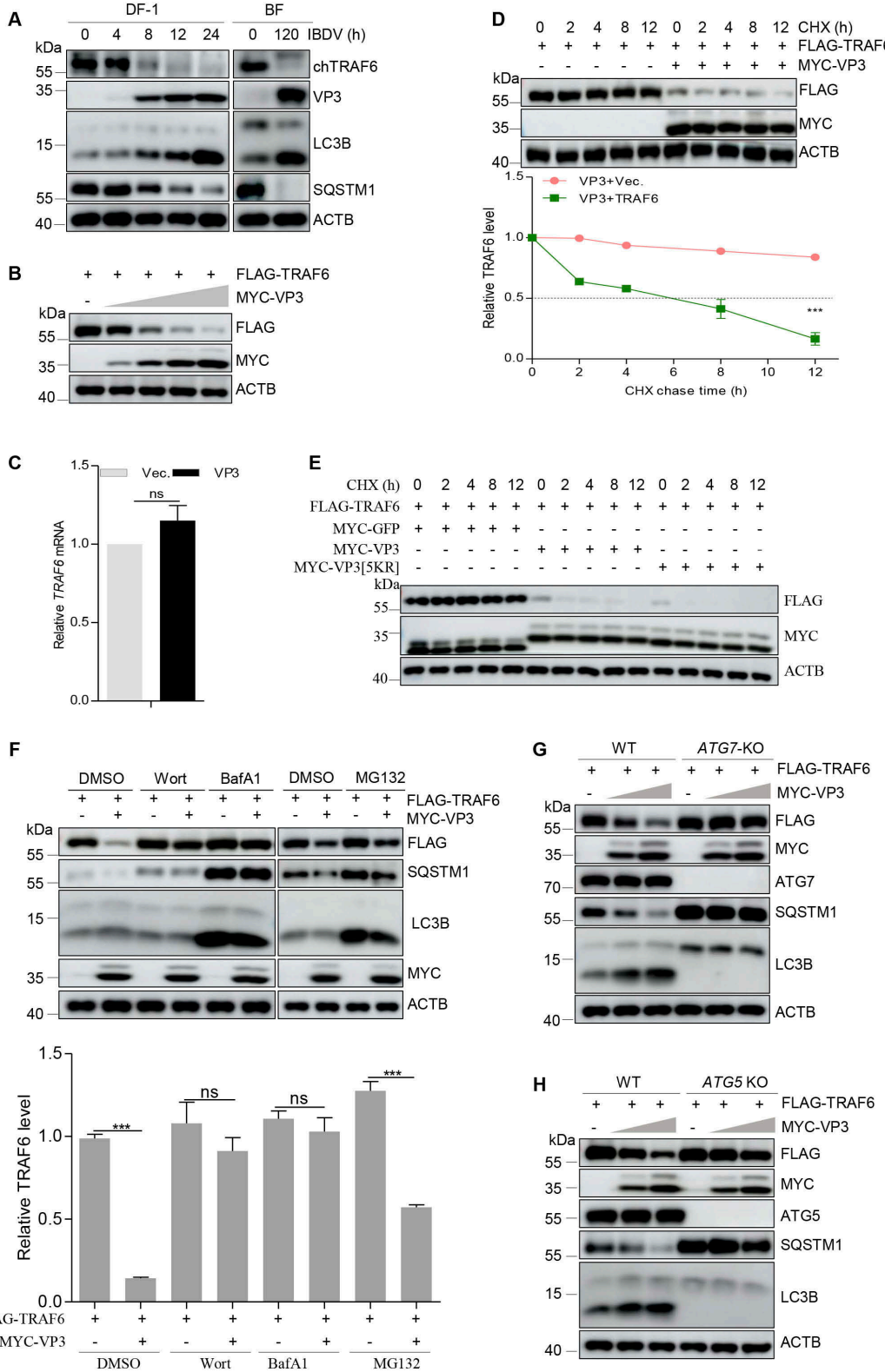

Figure 6. VP3 facilitates TRAF6 autophagic degradation. (**A**) IBDV infection induced autophagy and decrease of TRAF6 expression *in vitro* and *in vivo*. DF-1 cells were infected with IBDV strain CT (MOI = 10) for indicated time. Two-week-old SPF chickens were infected with IBDV strain CT ($10^{6.5}$ $TCID_{50}$/0.2 ml) for 120 h and chicken<apos;>s bursa was collected. (**B**) VP3 decreases TRAF6 levels in a dose-dependent manner. Vectors expressing FLAG-TRAF6 and MYC-VP3 or the corresponding empty vector were co-transfected into 293 T cells for 24 h. (**C**) VP3 has no significant impact on mRNA transcript level of *TRAF6*. Vectors expressing MYC-VP3 or corresponding empty vector was transfected separately into 293 T cells for 24 h. Cellular lysates were subjected to RT-PCR as described in the Materials and methods. (**D**) VP3 overexpression shortens the half-life of TRAF6. Vectors expressing FLAG-TRAF6 and MYC-VP3 or the corresponding empty vector were co-transfected into 293 T cells for 24 h. The resultant cells were treated with cycloheximide (CHX, 100 μg/ml). (**E**) The effects of WT and 5KR mutant VP3 on TRAF6 stability. 293 T cells were co-transfected with vectors expressing FLAG-TRAF6 (500 ng) and MYC-VP3 (500 ng), its mutant 5KR (1 μg) or control vector MYC-GFP for 24 h, and then treated with CHX for the indicated time. (**F**) VP3 facilitates TRAF6 autophagic degradation. Vectors expressing FLAG-TRAF6 and MYC-VP3 or empty vector were co-transfected into 293 T cells for 36 h, followed by treatment for 12 h with autophagosomal inhibitors, bafilomycin A_1 (100 nM) or wortmannin (10 μM) and ubiquitin proteasome inhibitor, MG132 (10 μM). (**G** and **H**) Immunoblotting analysis of FLAG-TRAF6 in cellular lysates from WT, *ATG7* (G) or *ATG5* (H) knockout cells transfected with vectors expressing MYC-VP3. WT, *ATG7* or *ATG5* knockout 293 T cells were co-transfected with vectors expressing FLAG-TRAF6 and different doses of MYC-VP3 for 36 h. Cellular lysates of samples from (A), (B) and (D-H) were subjected to western blotting using the indicated antibodies. ACTB levels served as a loading control.

autophagy receptor SQSTM1 to downregulate its expression for ensuring viral propagation. In present study, *Avibirnavirus* infection induced decreased TRAF6 levels by VP3 targeting autophagic adaptor SQSTM1. Considering these data, whether viral protein VP4 also binds SQSTM1 to induce TRAF6-autophagic degradation during *Avibirnavirus* infection deserves further investigation.

In summary, our findings demonstrated that *Avibirnavirus* VP3 could be ubiquitinated at the Lys residues 73, 135, 158, 193, and 219. Ubiquitin chains conjugated to the Lys residues 73, 135,193, and 219 on VP3 played an essential role in ensuring IBDV replication. In addition, the zinc finger domain of TRAF6 interacted with VP3 and mediated K11- and K33-linked ubiquitination of VP3 to enhance its nuclear accumulation, resulting in the inhibition of SUMOylated API5-mediated IFNB production and the increase of viral replication. Meanwhile, VP3 induced TRAF6 selective autophagy degradation by enhancing the recognition of TRAF6 by SQSTM1, leading to the inhibition of TRAF6-mediated NFKB activation and IFNB production (Figure 8).

Materials and methods

Cells and viruses

DF-1 (ATCC, CRL-12203) and HEK293T (ATCC, CRL-11268,) cells were cultured in Dulbecco<apos;>s modified Eagle<apos;>s medium (DMEM; Gibco, 12,100–038) containing 10% fetal bovine serum (FBS). BSRT cells stably expressing T7 RNA polymerase and IBDV strain CT have been described previously [32].

Antibodies and reagents

Anti-ATG5 (ET1611-38), anti-ATG7 (ET1610-53), anti-RELA /p65 (ET1603-12), and anti-CHUK/IKKα-IKBKB/IKKβ (ET1611-23) rabbit monoclonal antibodies (mAbs), anti-HISTONE H3 (M1306-4) and anti-ACTB/β-actin (M1210-2) mouse mAbs and anti-MYC (R1208-1) and anti-FLAG (0912–1) rabbit polyclonal antibodies (pAbs) were obtained from Hangzhou HuaAn Biotechnology. Anti-phospho-RELA/p65 (3033S), anti-phospho-CHUK/IKKα-IKBKB/IKKβ (2697S) and anti-LC3B (2775S) rabbit mAbs, and anti-ubiquitin (3936S) mouse mAbs were purchased from Cell Signaling Technology. Anti-SQSTM1 (18,420-1-AP) rabbit pAbs were provided by Proteintech. Anti-SQSTM1(ab109012) rabbit mAb for against chicken SQSTM1 was obtained from Abcam. Anti-GAPDH (glyceraldehyde-3-phosphate dehydrogenase) rabbit pAbs (AB-P-R001) were purchased from GoodHere Biotechnology. Anti-FLAG (F1804), anti-MYC (M5546), and anti-HA (H3663) mouse mAbs were purchased from Sigma-Aldrich. Mouse mAbs against IBDV viral proteins VP1 (1D4), VP2 (4C12), VP3 (2D6), VP4 (6 H8), and VP5 (5C1) and anti-chickenTRAF6 (chTRAF6) rabbit pAbs were generated and stored in our laboratory [30,72–74].

Cycloheximide (CHX; HY-12320) and bafilomycin A_1 (HY-100558) were purchased from MedChemExpress. Wortmannin (12–338) and N-ethylmaleimide (NEM; E3876) were supplied by Sigma-Aldrich. MG132 (S1748-5 mg), NP-40 lysis buffer (P0013 F), ATP (D7378-1 ML) and the dual luciferase reporter gene assay kit (RG028) were purchased from Beyotime Biotechnology. Phenylmethylsulfonyl fluoride (PMSF; P8340) and 1,4-dithio-DL-threitol (DTT; 3483–12-3) were purchased from Solarbio. G418 (ant-gn-1), poly (I:C) (tlrl-picw), and puromycin (58–58-2) were purchased from InvivoGene. The RevertAid RT reverse transcription kit (K1622) was obtained from Thermo Fisher Scientific. Biobest transfection reagents (BB0002) were provided by BioBEST Biotechnology. Protein A/G PLUS-Agarose (sc-2003) was purchased from Santa Cruz Biotechnology. RQ1 RNase-Free DNase (M6101) was purchased from Promega. The PrimeScript™ RT reagent Kit with gDNA Eraser (Perfect Real Time) (RR047A) and TB Green® Premix Ex Taq™ (Tli RNaseH Plus) (RR420A) were purchased from Takara.

Constructs

Dual luciferase reporter plasmid *IFNB* was generously provided by Prof. Jihui Ping from the Nanjing Agricultural University. Reporter plasmid *NFKB* (D2206) was purchased from Beyotime Biotechnology. *TRAF6* ORFs amplified from DF-1 and 293 T cells were separately inserted into vector pCMV-FLAG-N vector (Clontech, 635,688) or pCMV-MYC -N vector (Clontech, 635,689) designed as *FLAG*-ch*TRAF6, FLAG-TRAF6* and *MYC-TRAF6*, respectively. Vectors expressing MYC-SQSTM1 and FLAG-tagged autophagy receptors (SQSTM1, OPTN, CALCOCO2/NDP52, NBR1, and TAX1BP1), *MYC-VP3*, rescued plasmid IBDV strain CT *T7-A* and *T7-B, HA-Ub, HA-UbK48*, and *HA-UbK63* were stored in our laboratory. *MYC-SQSTM1*-(T2, T3, T4) and *FLAG-TRAF6, pET-32A-TRAF6* and *FLAG*-ch*TRAF6* mutants were constructed by mutation using the WT plasmid as the template. *MYC-SQSTM1*-T1 or T5 and FLAG-tagged *TRAF3, RNF125, RNF135, TRIM25, UBE2D2* and *UBE2D3* were generated by standard molecular biology techniques. Except for *UBE2D2* and *UBE2D3*, the expression plasmids of human FLAG-tagged E2 conjugated enzymes were constructed by ClonExpress MultiS One Step Cloning Kit (Vazyme Biotech Co., Ltd, C113-02). Several mutants of *MYC-VP3*, rescued plasmid *T7-A*, and *HA-Ub* were constructed by site-specific mutation experiments. All primers used are summarized in Table S1.

Virus infection and western blotting

DF-1 cells were mock-infected or infected with IBDV at a multiplicity of infection (MOI) of 10. At different time points, cells were harvested and lysed in Radioimmunoprecipitation assay (RIPA) lysis buffer (Beyotime Biotechnology, P0013C). Protein samples were prepared and separated by SDS-PAGE, followed by transfer to nitrocellulose blotting membranes (GE Healthcare Life Science, 10,600,001). After blocking with 5% skim milk containing 0.1% Tween 20 (Amresco, 0777–1 L) for 1 h at room temperature, the membranes were washed three times with phosphate-buffered saline (PBS; 137 mM NaCl [Sinopharm Chemical Reagent Co., Ltd, 10,019,318], 10 mM Na_2HPO_4 [Sinopharm Chemical Reagent Co., Ltd, 10,020,318], 1.8 mM

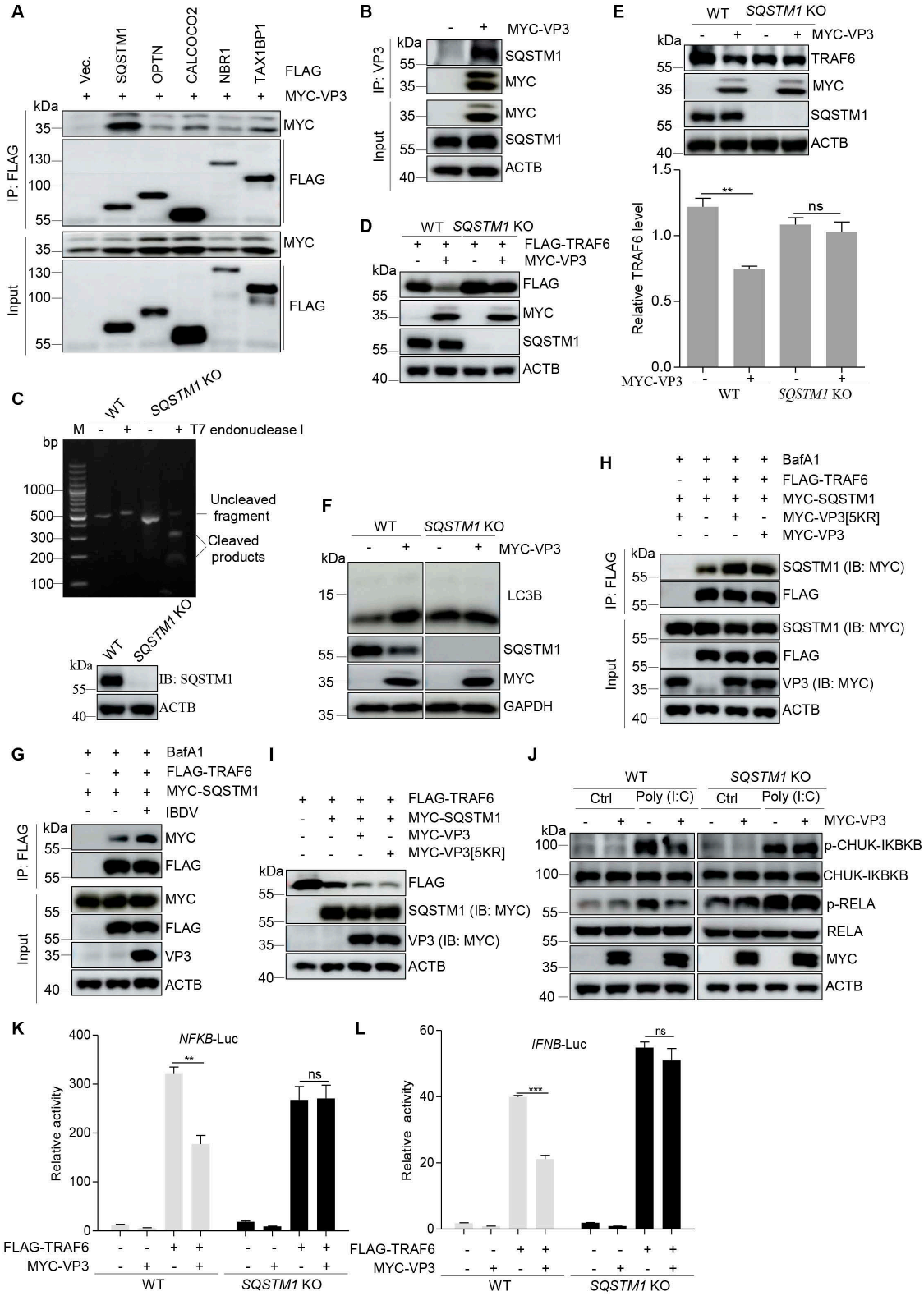

Figure 7. VP3 blocks TRAF6-mediated NFKB activation by SQSTM1-targeted TRAF6 autophagic degradation. (**A** and **B**) VP3 interacts strongly with SQSTM1, but not with OPTN, CALCOCO2, NBR1, and TAX1BP1. Vectors expressing MYC-VP3 and different FLAG-tagged autophagy receptors were co-transfected into 293 T cells for 48 h, respectively (A). 293 T cells were transfected with *MYC-VP3* for 36 h (B). Cellular lysate samples from (A) and (B) were subjected to an immunoprecipitation assay using anti-FLAG mouse mAbs or anti-VP3 mouse mAbs, followed by an immunoblotting assay using the indicated antibodies. (**C**) Generation of *SQSTM*1 knockout 293 T cells. The genomic DNA and cellular lysates from WT or *SQSTM1* knockout 293 T cells were subjected to T7 endonuclease I (upper) and western blotting assays with anti-SQSTM1 rabbit pAbs (bottom). (**D** and **E**) VP3 promotes TRAF6 degradation in autophagic receptor SQSTM1-dependent manner. WT or *SQSTM1* knockout 293 T cells were transfected with vectors expressing FLAG-TRAF6 and MYC-VP3 (D) or MYC-VP3 alone (E) for 36 h. Cellular lysates were subjected to western blotting analysis using the indicated antibodies. (**F**) IBDV VP3 induced receptor SQSTM1-mediated selective autophagy. WT and *SQSTM1* knockout cells were separately transfected with *MYC-VP3* or corresponding empty vector for 42 h, the lysates were subjected to western blotting assays with indicated antibodies. GAPDH served as loading control. (**G**) 293 T cells were co-transfected with vectors expressing FLAG-TRAF6 and MYC-SQSTM1 for 30 h, followed by IBDV infection and autophagic inhibitor BafA1 (200 nM) treatment for 12 h. The lysates were immunoprecipitated using anti-FLAG mouse mAbs and immunoblotted using the indicated antibodies.

KH_2PO_4 [Sinopharm Chemical Reagent Co., Ltd, 10,017,618], pH 7.4), 2.7 mM KCl [Sinopharm Chemical Reagent Co., Ltd, 10,016,318] containing 0.1% Tween 20 (Amresco, 0777–1 L) and then incubated with the indicated primary antibodies overnight at 4°C. Next day, the blots were incubated with horseradish peroxidase-conjugated goat anti-mouse/rabbit IgG (Kirkegaard & Perry Laboratories, Inc., 074–1506). Protein bands were then visualized using a SuperSignal West Femto Substrate Trial Kit (Thermo Fisher Scientific/Pierce, 34,095) and imaged using AI680 Images (GE Health Care).

IBDV virion purification

Sucrose (Sinopharm Chemical Reagent Co.,Ltd, 10,021,418) density gradient centrifugation was performed. DF-1 cells were infected with IBDV (MOI = 0.01) and harvested when the cytopathic effect was obviously displayed. After freeze-thawing three times, the cellular lysates were collected and centrifuged at 6,000 × *g* for 10 min. The supernatants were then ultra-centrifuged at 160,000 × *g* for 1.5 h at 4°C using an Optima L-100XP ultracentrifuge (Beckman Coulter). The pellets were soaked with PBS (137 mM NaCl [Sinopharm Chemical Reagent Co., Ltd, 10,019,318], 2.7 mM KCl [Sinopharm Chemical Reagent Co., Ltd, 10,016,318], 10 mM Na_2HPO_4 [Sinopharm Chemical Reagent Co., Ltd, 10,020,318], 1.8 mM KH_2PO_4 [Sinopharm Chemical Reagent Co., Ltd, 10,017,618], pH 7.4) overnight at 4°C, and then resuspended. Subsequently, the viral suspension after centrifugation at 10,000 × *g* for 10 min at 4°C was transferred to Ultra-Clear centrifuge tubes (Beckman Coulter, 344,057). Sucrose solutions at various concentrations of 30% to 60% were prepared. Then, 1 ML of 30%, 40%, 50%, and 60% sucrose working solution were added sequentially to the bottom of the tube to form a density gradient. Samples were added on the top of the gradient, and then centrifuged at 133, 900 × *g* for 3.5 h at 4°C. Fractions at different sucrose concentration interfaces were collected. Finally, purified IBDV particles were subjected to 12% SDS-PAGE followed by Coomassie Brilliant Blue R250 staining.

Protein expression and purification

The plasmids *pGEX-4 T-1-VP3, pET-28A-TRAF6, pET-32A-TRAF6, pET-32A-TRAF6*^{C70A}, *pET-32A-UBA1* and *pET-32A-UBE2D1* were transformed into *Escherichia coli* BL21 (pLysS; Sangon Biotechnology, B528415-0010) competent cells, respectively, and then induced with 1 mM IPTG (Sangon Biotechnology, A600168-0025) at 16°C with shaking at 90 rpm, overnight. After centrifugation, the pellets were lysed in binding buffer by sonication. After centrifugation at 12,000 × *g* for 10 min at 4°C, HIS-tagged recombinant proteins, GST, and GST-VP3 in the supernatants were purified using Ni-NTA agarose (QIAGEN, 30,210) and Glutathione (GST) Resin (GenScript, L00206) according to manufacturer<apos;>s instructions and eluted in elution buffer. For HIS-tagged recombinant proteins, the binding buffer was 50 mM Tri-HCl, pH 8.0, 10 mM imidazole; and the elution buffer was binding buffer containing 80 mM imidazole. For GST and GST-VP3, the binding buffer was 50 mM Tri-HCl, pH 8.0, 150 mM NaCl; and the elution buffer was binding buffer containing 10 mg/5 ml reduced glutathione (Sangon Biotechnology, A100399-0005).

Co-immunoprecipitation and GST affinity-isolation assays

For the co-IP assay, cells were lysed in NP-40 lysis buffer containing PMSF for 4 h. After centrifugation at 12,000 × *g* for 10 min at 4°C, the supernatants were incubated with the indicated antibodies and protein A/G PLUS-agarose for 4 h at 4°C. For the GST affinity-isolation assay, purified GST (10 μg) and GST-VP3 (10 μg) recombinant proteins were separately mixed with purified HIS-TRAF6 (20 μg) in 500 μL NP-40 lysis buffer for 4 h at 4°C, followed by adding the GST resin. After centrifugation at 1,000 × *g* for 5 min at 4°C, the pellets were washed with NP-40 lysis buffer and then lysed in RIPA lysis buffer (Beyotime Biotechnology, P0013B) for immunoblotting analysis.

Mass spectrometry (MS)

To determine the ubiquitinated sites on viral protein VP3, *MYC-VP3* was transfected into 293 T cells. At 48 h after transfection, the cells were harvested and lysed in NP-40 lysis buffer containing PMSF and N-ethylmaleimide (NEM) for 4 h at 4°C. The supernatants were subjected to an immunoprecipitation assay using anti-MYC mouse mAbs. The immunoprecipitation complexes were subjected to SDS-PAGE and Coomassie Brilliant Blue R250 staining. Subsequently, the regions of the staining gels beyond 25 kDa were mixed together and subjected to Liquid Chromatography Mass Spectrometry (LC-MS) analysis in APTBio (Shanghai, China) to identify the specific ubiquitinated sites of VP3.

Cellular fractionation

The process has been described previously [75].

Indirect immunofluorescence assay (IFA)

Mock-infected or IBDV-infected DF-1 cells were fixed with an equal volume of methanol and acetone for 30 min at –

(**H**) Vectors expressing FLAG-TRAF6, MYC-SQSTM1, and MYC-VP3 or its mutant 5KR were co-transfected into 293 T cells. At 30 h after transfection, the cells were treated with BafA1 (200 nM) for 12 h. The cellular lysates were used for immunoprecipitation and immunoblotting assays with the indicated antibodies. (**I**) 293 T cells were co-transfected with vectors expressing FLAG-TRAF6, MYC-SQSTM1, or empty vector, and MYC-VP3 or its mutant 5KR for 36 h. The lysates were subjected to western blotting assays using the indicated antibodies. (**J**) The inhibition of NFKB activation by VP3 is SQSTM1-dependent. WT and *SQSTM1* knockout cells were transfected with vectors expressing MYC-VP3 or the corresponding empty vector for 36 h, followed by stimulation with poly (I:C) (1 μg) for 8 h. Cellular lysates were immunoblotted using phospho-CHUK-IKBKB, CHUK-IKBKB, phospho-RELA and RELA rabbit pAbs. (**K** and **L**) Luciferase assays of the *IFNB* or *NFKB* promoter. WT and *SQSTM1* knockout 293 T cells were co-transfected with the *IFNB* or *NFKB* reporter plasmids along with *FLAG-TRAF6* in the presence or absence of the plasmid encoding VP3.

20°C, and then were incubated with anti-VP2 mouse mAbs overnight at 4°C. After washing three times with PBS (137 mM NaCl [Sinopharm Chemical Reagent Co., Ltd, 10,019,318], 2.7 mM KCl [Sinopharm Chemical Reagent Co., Ltd, 10,016,318], 10 mM Na2HPO4 [Sinopharm Chemical Reagent Co., Ltd, 10,020,318], 1.8 mM KH2PO4 [Sinopharm Chemical Reagent Co., Ltd, 10,017,618], pH 7.4), the cells were incubated with fluorescein isothiocyanate (FITC)-conjugated goat anti-mouse IgG (Kirkegaard & Perry Laboratories, Inc., 172–1806) for 1 h at room temperature. After washing five times with PBS, the fluorescence signal was scanned under a fluorescence microscope (OLYMPUS, U-RFL-T).

Virus rescue

Recombinant IBDV strain CT possessing wild-type (WT) or K73R, K158R, K193R, or K219R mutant VP3 (designated as rWT, rK73R, rK158R, rK193R, and rK219R) were generated by reverse genetics, as described previously [15]. Briefly, WT or several mutants *T7-A* clones together with *T7-B* were co-transfected separately into BSRT7 cells for 72 h, with *T7-A* alone as a negative control. After freeze-thawing, cellular lysates after were centrifugated at 6, 000 × *g* for 10 min, and the supernatants were transferred into fresh DF-1 cells. At 3 h after infection, the supernatants were removed, followed by adding fresh DMEM containing 2% FBS for continuous culture for another 48 h.

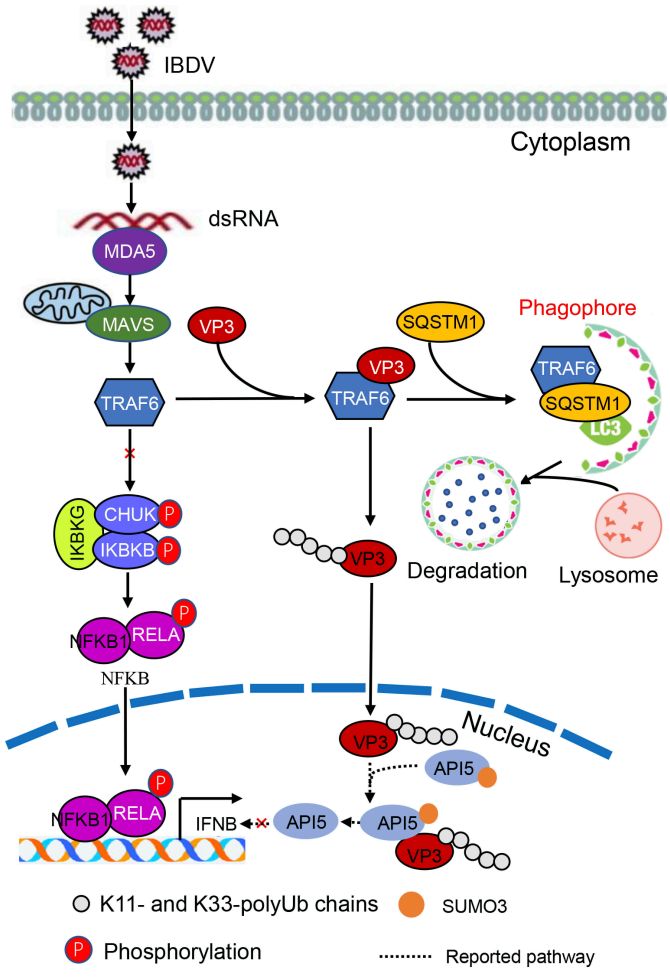

Figure 8. The proposed model by which IBDV VP3 supports virus replication through hijacking TRAF6 and inactivating the NFKB pathway. TRAF6 targeted VP3 and mediated its K11- and K33-polyubiquitination, which contributed to increase VP3 nuclear accumulation for inhibiting SUMOylated API5-mediated IFNB production. Additionally, IBDV VP3 could promote TRAF6 selective autophagic degradation in a SQSTM1-dependent manner by enhancing the recognition by autophagic receptor SQSTM1 of TRAF6, leading to the inhibition of NFKB activity and IFNB production. These two strategies were employed by IBDV VP3 to create an environment conducive to efficient viral proliferation.

Viral titer detection

DF-1 cells were infected with IBDV (MOI = 10). At different time points after infection, cells were harvested and freeze-thawed three times. After centrifugation at 12,000 × *g* for 10 min at 4°C, the supernatants were subjected to $TCID_{50}$ (50% tissue culture infective dose) detection. Briefly, the viral suspension was diluted 10-fold using DMEM containing 2% FBS, and then added to fresh DF-1 cells. Eight repeats of each diluted sample were tested. At 48 h after infection, the cells were subjected to an IFA assay with anti-VP2 mouse mAbs. Virus titers were determined by observing the infected cells under a fluorescence microscope (OLYMPUS, U-RFL-T) and calculating the $TCID_{50}$ per 0.1 ML.

Reverse transcription PCR (RT-PCR) and quantitative real time reverse transcription PCR (qRT-PCR)

For RT-PCR, total RNA was extracted and 1 μg of RNA treated by RNase-Free Dnase was reverse-transcribed into cDNA using a RevertAid RT reverse transcription kit (Thermo Fisher Scientific, K1622). Subsequently, *VP3* and *GAPDH* mRNAs were amplified using 2 × Taq Master Mix (Vazyme Biotech Co., Ltd, P114-01). The PCR products were separated on 1.5% nucleic acid agarose gels, and the images were scanned using a Gel Documentation system (GenoSens 1880). For qRT-PCR, total RNA was extracted and reverse-transcribed into cDNA using PrimeScript™ RT reagent Kit with gDNA Eraser according to the manufacturer<apos;>s protocols. The cDNA was subjected to qPCR using TB Green® Premix Ex Taq™. The expression of *ACTB/β-actin* was used to normalize the relative abundance of indicated gene mRNA. The primers used are listed in Table S1.

CRISPR-Cas9 knockout

The *TRAF6* gene target sequence (5′-TACTATACT CATCCAGAGAAC-3′), *ATG5* gene target sequence (5′-AAATGTACTGTGATGTTCCA-3′), *ATG7* gene target sequence (5′-AGAAGAAGCTGAACGAGTAT-3′), and *SQSTM1* gene target sequence (5′-AGGGCTTCTC GCACAGCCGC-3′) were inserted separately into the guide RNA expression plasmid PX459 (Addgene, 62,988; deposited by Feng Zhang). The recombinant constructs were transfected separately into 293 T cells. At 36 h after transfection, the cells were selected using puromycin (10 μg/ml) for 48 h. Finally, the monoclonal cells were obtained using the limiting dilution method. T7 Endonuclease (Vazyme Biotech Co., Ltd, EN303-01) and immunoblotting assays were used to identify

monoclonal cell lines. The primers used for PCR amplification are listed Table S2.

Luciferase activity assay

293 T cells were transfected with luciferase reporter plasmids (*NFKB* and *IFNB*), pRL-TK, and the indicated plasmids. At 36 h after transfection, the cells were harvested, and luciferase activity was detected using a dual luciferase reporter kit according to the manufacturer<apos;>s instructions. All experiments were repeated at least three times.

In vitro ubiquitination assay

HIS-tagged E1(UBA1), UBE2D1, ubiquitin, TRAF6, $TRAF6^{C70A}$ and GST-VP3 proteins were purified from *E. coli*. Subsequently, *in vitro* ubiquitination assay was conducted as described previously [76]. Briefly, 500 μL of ubiquitination buffer (20 mM Tris-HCl, pH 7.5, 5 mM $MgCl_2$, 2 mM DTT, supplemented with 2 mM ATP) was mixed with ubiquitin (50 μg), UBA1 (2 μg), UBE2D1 (3 μg), TRAF6 or $TRAF6^{C70A}$ (8 μg) and GST-VP3 (20 μg). The mixture was incubated at 37°C for 2 h, and followed by GST affinity-isolation assay. Finally, the sample was washed using 1 M urea for 60 min to exclude potential binding of unanchored polyubiquitin, then the sample was placed in SDS-loading buffer and boiled for 10 min. Samples were fractionated on 8% SDS-PAGE followed by western blotting with anti-ubiquitin mAb.

Animal experiments

Eighteen 2-week-old SPF chickens were randomly divided into six groups and infected with viruses at a dose of 0.2 ml ($10^{6.5}$ $TCID_{50}$/0.2 ml), respectively, to detect the replication characteristics of the rWT and different mutant viruses *in vivo*. The inoculated chickens were bled and sacrificed at 5 days post-infection (dpi). Bursae of chickens were collected and weighed. Viral loads in bursal tissues were detected using the primer targeting the IBDV B segment (Table S1) by RT-qPCR as described previously [77]. Simultaneously, bursae were fixed by immersion in 4% neutral formaldehyde, sliced and stained with hematoxylin and eosin for further histopathological examination.

Acknowledgments

This study is supported by grants from National Natural Science Foundation of China (Grant No.31630077) and China Agriculture Research System (Grant No. CARS-40-K13).

Disclosure statement

No potential conflict of interest was reported by the author(s).

Funding

This work was supported by the Agriculture Research System of China [CARS-40-K13]; National Natural Science Foundation of China [31630077].

Statistical analysis

Statistical differences were assessed using one-way ANOVAs using IBM SPSS Statistics 20 (IBM Corp., Armonk, NY, USA). All data are presented as the mean ± SD of three independent experiments. For all experiments, $p < 0.05$ was considered statistically significant. In the figures * $p< 0.05$, ** $p < 0.01$, *** $p < 0.001$, not significant (ns): $p > 0.05$.

References

[1] He X, Zhu Y, Zhang Y, et al. RNF34 functions in immunity and selectivemitophagy by targeting MAVS for autophagic degradation. EMBO J. 2019;38(14):e100978. DOI:10.15252/embj.2018100978.
[2] Yang W L, Wang J, Chan C H, et al. The E3 ligase TRAF6 regulates Akt ubiquitination and activation. Science. 2009;325(5944):1134–1138. DOI:10.1126/science.1175065.
[3] Choi YB, Harhaj EW, Ross SR. HTLV-1 tax stabilizes MCL-1 via TRAF6-dependent K63-linked polyubiquitination to promote cell survival and transformation. PLoS Pathog. 2014;10(10):e1004458.
[4] Ni X, Kou W, Gu J, et al. TRAF6 directs FOXP3 localization and facilitates regulatory T-cell function through K63-linked ubiquitination. EMBO J. 2019;38(9):e99766. DOI:10.15252/embj.201899766.
[5] Dynek J N, Goncharov T, Dueber E C, et al. c-IAP1 and UbcH5 promote K11-linked polyubiquitination of RIP1 in TNF signalling. EMBO J. 2010;29(24):4198–4209. DOI:10.1038/emboj.2010.300.
[6] Ciechanover A. The unravelling of the ubiquitin system. Nat Rev Mol Cell Biol. 2015;16(5):322–324.
[7] Heaton SM, Borg NA, Dixit VM. Ubiquitin in the activation and attenuation of innate antiviral immunity. J Exp Med. 2016;213(1):1–13.
[8] Komander D, Rape M. The ubiquitin code. Annu Rev Biochem. 2012;81(1):203–229.
[9] Li Z, Wang Y, Li Y, et al. Ube2s stabilizes β-Catenin through K11-linked polyubiquitination to promote mesendoderm specification and colorectal cancer development. Cell Death Dis. 2018;9(5):456. DOI:10.1038/s41419-018-0451-y.
[10] Meng Y, Liu C, Shen L, et al. TRAF6 mediates human DNA2 polyubiquitination and nuclear localization to maintain nuclear genome integrity. Nucleic Acids Res. 2019;47(14):7564–7579. DOI:10.1093/nar/gkz537.
[11] Peng S J, Yao R R, Yu S S, et al. UBL4A augments innate immunity by promoting the K63-linked ubiquitination of TRAF6. J Immunol. 2019;203(7):1943–1951. DOI:10.4049/jimmunol.1800750.
[12] Huang H, S JM, Liao L, et al. K33-linked polyubiquitination of T cell receptor-zeta regulates proteolysis-independent T cell signaling. Immunity. 2010;33(1):60–70. DOI:10.1016/j.immuni.2010.07.002.
[13] M YL, Manfiolli A O, Denadai-Souza A, et al. Tumor necrosis factor receptor-associated factor 6 interaction with alpha-synuclein enhances cell death through the Nuclear Factor-kB pathway. IBRO Rep. 2020;9:218–223.
[14] Zhang L, Wei N, Cui Y, et al. The deubiquitinase CYLD is a specific checkpoint of the STING antiviral signaling pathway. PLoS Pathog. 2018;14(11):e1007435. DOI:10.1371/journal.ppat.1007435.
[15] Wu H, Shi L, Zhang Y, et al. Ubiquitination is essential for avibirnavirus replication by supporting VP1 polymerase activity. J Virol. 2019;93(3):e01899–18. DOI:10.1128/JVI.01899-18.

[16] Fu B, Wang L, Ding H, et al. TRIM32 senses and restricts influenza a virus by ubiquitination of PB1 polymerase. PLoS Pathog. 2015;11(6):e1004960. DOI:10.1371/journal.ppat.1004960.

[17] Patil G, Zhao M, Song K, et al. TRIM41-mediated ubiquitination of nucleoprotein limits influenza A virus infection. J Virol. 2018;92(16):e00905–18. DOI:10.1128/JVI.00905-18.

[18] Su W-C, Y W-Y, H S-H, et al. Ubiquitination of the cytoplasmic domain of influenza a virus m2 protein is crucial for production of infectious virus particles. J Virol. 2018;92(4):e01972–17. DOI:10.1128/JVI.01972-17.

[19] L LT, Y WC, C SW, et al. Ubiquitination and deubiquitination of NP protein regulates influenza A virus RNA replication. EMBO J. 2010;29(22):3879–3890. DOI:10.1038/emboj.2010.250.

[20] Wang T, Du Q, Wu X, et al. Porcine MKRN1 modulates the replication and pathogenesis of porcine circovirus type 2 by inducing capsid protein ubiquitination and degradation. J Virol. 2018;92(11):e00100–18.

[21] Bharaj P, Atkins C, Luthra P, et al. The host E3-Ubiquitin Ligase TRIM6 Ubiquitinates the Ebola Virus VP35 protein and promotes virus replication. J Virol. 2017;91(18):e00833–17. DOI:10.1128/JVI.00833-17.

[22] Li L, Bai J, Fan H, et al. E2 ubiquitin-conjugating enzyme UBE2L6 promotes Senecavirus A proliferation by stabilizing the viral RNA polymerase. PLoS Pathog. 2020;16(10):e1008970. DOI:10.1371/journal.ppat.1008970.

[23] M SJ, J KI, Rautenschlein S, et al. Infectious bursal disease virus of chickens: pathogenesis and immunosuppression. Dev Comp Immunol. 2000;24(2–3):223–235. DOI:10.1016/S0145-305X(99)00074-9.

[24] Muller H, Scholtissek C, Becht H. The genome of infectious bursal disease virus consists of two segments of double-stranded RNA. J Virol. 1979;31(3):584–589.

[25] Wang S, Hu B, Si W, et al. Avibirnavirus VP4 Protein Is a Phosphoprotein and partially contributes to the cleavage of intermediate precursor VP4-VP3 Polyprotein. PLoS One. 2015;10(6):e0128828. DOI:10.1371/journal.pone.0128828.

[26] Hu B, Zhang Y, Jia L, et al. Binding of the pathogen receptor HSP90AA1 to avibirnavirus VP2 induces autophagy by inactivating the AKT-MTOR pathway. Autophagy. 2015;11(3):503–515. DOI:10.1080/15548627.2015.1017184.

[27] Zheng X, Hong L, Shi L, et al. Proteomics analysis of host cells infected with infectious bursal disease virus. Mol Cell Proteomics. 2008;7(3):612–625. DOI:10.1074/mcp.M700396-MCP200.

[28] Ferrero D, Garriga D, Navarro A, et al. Infectious Bursal Disease Virus VP3 Upregulates VP1-Mediated RNA-Dependent RNA replication. J Virol. 2015;89(21):11165–11168. DOI:10.1128/JVI.00218-15.

[29] Lombardo E, Maraver A, R CJ, et al. VP1, the putative RNA-dependent RNA polymerase of infectious bursal disease virus, forms complexes with the capsid protein VP3, leading to efficient encapsidation into virus-like particles. J Virol. 1999;73(8):6973–6983. DOI:10.1128/JVI.73.8.6973-6983.1999.

[30] Ye C, Jia L, Sun Y, et al. Inhibition of antiviral innate immunity by birnavirus VP3 protein via blockage of viral double-stranded RNA binding to the host cytoplasmic RNA detector MDA5. J Virol. 2014;88(19):11154–11165. DOI:10.1128/JVI.01115-14.

[31] Zhang Y, Hu B, Li Y, et al. Binding of Avibirnavirus VP3 to the PIK3C3-PDPK1 complex inhibits autophagy by activating the AKT-MTOR pathway. Autophagy. 2020;16(9):1697–1710. DOI:10.1080/15548627.2019.1704118.

[32] Wu H, Yang H, Ji G, et al. SUMO1 modification facilitates avibirnavirus replication by stabilizing polymerase VP1. J Virol. 2019;93(10):e02227–18. DOI:10.1128/JVI.02227-18.

[33] Pan J, Lin L, Tao YJ. Self-guanylylation of birnavirus VP1 does not require an intact polymerase activity site. Virology. 2009;395(1):87–96.

[34] Zhang Y, F LL, Munir M, et al. RING-Domain E3 Ligase-Mediated Host-Virus interactions: orchestrating immune responses by the host and antagonizing immune defense by viruses. Front Immunol. 2018;9:1083.

[35] U GM, A AR, Urano T, et al. Influenza A virus NS1 targets the ubiquitin ligase TRIM25 to evade recognition by the host viral RNA sensor RIG-I. Cell Host Microbe. 2009;5(5):439–449. DOI:10.1016/j.chom.2009.04.006.

[36] Nailwal H, Sharma S, K MA, et al. The nucleoprotein of influenza A virus induces p53 signaling and apoptosis via attenuation of host ubiquitin ligase RNF43. Cell Death Dis. 2015;6(5):e1768. DOI:10.1038/cddis.2015.131.

[37] Yan J, C SM, Hao C, et al. HIV-1 Vpr Reprograms CLR4(DCAF1) E3 Ubiquitin Ligase to Antagonize Exonuclease 1-Mediated Restriction of HIV-1 Infection. mBio. 2018;9(5):e01732–18. DOI:10.1128/mBio.01732-18.

[38] Bauer M, W FJ, Seiler D, et al. The E3 ubiquitin ligase mind bomb 1 controls adenovirus genome release at the nuclear pore complex. Cell Rep. 2019;29(12):3785–3795 e8. DOI:10.1016/j.celrep.2019.11.064.

[39] Kumar S, Barouch-Bentov R, Xiao F, et al. MARCH8 ubiquitinates the hepatitis C virus nonstructural 2 protein and mediates viral envelopment. Cell Rep. 2019;26(7):1800–1814 e5. DOI:10.1016/j.celrep.2019.01.075.

[40] Min Y, J KM, Lee S, et al. Inhibition of TRAF6 ubiquitin-ligase activity by PRDX1 leads to inhibition of NFKB activation and autophagy activation. Autophagy. 2018;14(8):1347–1358. DOI:10.1080/15548627.2018.1474995.

[41] Kawai T, Akira S. TLR signaling. Cell Death Differ. 2006;13(5):816–825.

[42] Ninomiya-Tsuji J, Kishimoto K, Hiyama A, et al. The kinase TAK1 can activate the NIK-I kappaB as well as the MAP kinase cascade in the IL-1 signalling pathway. Nature. 1999;398(6724):252–256. DOI:10.1038/18465.

[43] Qian Y, Commane M, Ninomiya-Tsuji J, et al. IRAK-mediated translocation of TRAF6 and TAB2 in the interleukin-1-induced activation of NFkappa B. J Biol Chem. 2001;276(45):41661–41667. DOI:10.1074/jbc.M102262200.

[44] Takaesu G, Kishida S, Hiyama A, et al. TAB2, a novel adaptor protein, mediates activation of TAK1 MAPKKK by linking TAK1 to TRAF6 in the IL-1 signal transduction pathway. Mol Cell. 2000;5(4):649–658. DOI:10.1016/S1097-2765(00)80244-0.

[45] Deng L, Wang C, Spencer E, et al. Activation of the IkappaB kinase complex by TRAF6 requires a dimeric ubiquitin-conjugating enzyme complex and a unique polyubiquitin chain. Cell. 2000;103(2):351–361. DOI:10.1016/S0092-8674(00)00126-4.

[46] Lee S, Kim W, Ko C, et al. Hepatitis B virus X protein enhances Myc stability by inhibiting SCF(Skp2) ubiquitin E3 ligase-mediated Myc ubiquitination and contributes to oncogenesis. Oncogene. 2016;35(14):1857–1867. DOI:10.1038/onc.2015.251.

[47] Zheng N, Shabek N. Ubiquitin Ligases: structure, Function, and Regulation. Annu Rev Biochem. 2017;86(1):129–157.

[48] Akutsu M, Dikic I, Bremm A. Ubiquitin chain diversity at a glance. J Cell Sci. 2016;129(5):875–880.

[49] Di Pietro A, Kajaste-Rudnitski A, Oteiza A, et al. TRIM22 inhibits influenza A virus infection by targeting the viral nucleoprotein for degradation. J Virol. 2013;87(8):4523–4533. DOI:10.1128/JVI.02548-12.

[50] Li R, Chen C, He J, et al. E3 ligase ASB8 promotes porcine reproductive and respiratory syndrome virus proliferation by stabilizing the viral Nsp1alpha protein and degrading host IKKbeta kinase. Virology. 2019;532:55–68.

[51] Zhang Y, Zhang H, L ZG, et al. Porcine RING Finger Protein 114 inhibits classical swine fever virus replication via K27-linked polyubiquitination of viral NS4B. J Virol. 2019;93(21):e01248–19. DOI:10.1128/JVI.01248-19.

[52] Toma-Fukai S, Hibi R, Naganuma T, et al. Crystal structure of GCN5 PCAF N-terminal domain reveals atypical ubiquitin ligase structure. J Biol Chem. 2020;295(43):14630–14639. DOI:10.1074/jbc.RA120.013431.

[53] Khaminets A, Behl C, Dikic I. Ubiquitin-dependent and independent signals in selective autophagy. Trends Cell Biol. 2016;26(1):6–16.

[54] Geetha T, Wooten MW. Structure and functional properties of the ubiquitin binding protein p62. FEBS Lett. 2002;512(1–3):19–24.
[55] Bjorkoy G, Lamark T, Brech A, et al. p62/SQSTM1 forms protein aggregates degraded by autophagy and has a protective effect on huntingtin-induced cell death. J Cell Biol. 2005;171(4):603–614. DOI:10.1083/jcb.200507002.
[56] Pankiv S, H CT, Lamark T, et al. p62/SQSTM1 binds directly to Atg8/LC3 to facilitate degradation of ubiquitinated protein aggregates by autophagy. J Biol Chem. 2007;282(33):24131–24145. DOI:10.1074/jbc.M702824200.
[57] Zhang H, Zhang Y, Zhu X, et al. DEAD Box Protein 5 Inhibits Liver Tumorigenesis by Stimulating Autophagy via Interaction with p62/SQSTM1. Hepatology. 2019;69(3):1046–1063. DOI:10.1002/hep.30300.
[58] Lin YC, Jeng KS, Lai MMC. CNOT4-mediated ubiquitination of influenza a virus nucleoprotein promotes viral RNA replication. mBio. 2017;8(3):e00597–17. DOI:10.1128/mBio.00597-17.
[59] K BJ, M PG, Schorpp K, et al. Targeting TRAF6 E3 ligase activity with a small-molecule inhibitor combats autoimmunity. J Biol Chem. 2018;293(34):13191–13203. DOI:10.1074/jbc.RA118.002649.
[60] Deng T, Hu B, Wang X, et al. DeSUMOylation of apoptosis inhibitor 5 by avibirnavirus VP3 supports virus replication. mBio. 2021;12(4):e0198521. DOI:10.1128/mBio.01985-21.
[61] Schimmack G, Schorpp K, Kutzner K, et al. YOD1/TRAF6 association balances p62-dependent IL-1 signaling to NF-kappaB. Elife. 2017;6:e22416.
[62] B SR, Sun L, K EC, et al. Identification and characterization of MAVS, a mitochondrial antiviral signaling protein that activates NF-kappaB and IRF 3. Cell. 2005;122(5):669–682. DOI:10.1016/j.cell.2005.08.012.
[63] A KK, Abbas W, Varin A, et al. HIV-1 Nef interacts with HCV Core, recruits TRAF2, TRAF5 and TRAF6, and stimulates HIV-1 replication in macrophages. J Innate Immun. 2013;5(6):639–656. DOI:10.1159/000350517.
[64] Kitagawa Y, Yamaguchi M, Zhou M, et al. Human parainfluenza virus type 2 V protein inhibits TRAF6-mediated ubiquitination of IRF7 to prevent TLR7- and TLR9-dependent interferon induction. J Virol. 2013;87(14):7966–7976. DOI:10.1128/JVI.03525-12.
[65] Lv H, Dong W, Cao Z, et al. TRAF6 is a novel NS3-interacting protein that inhibits classical swine fever virus replication. Sci Rep. 2017;7(1):6737. DOI:10.1038/s41598-017-06934-1.
[66] Ye C, Yu Z, Xiong Y, et al. STAU1 binds to IBDV genomic double-stranded RNA and promotes viral replication via attenuation of MDA5-dependent beta interferon induction. FASEB J. 2019;33(1):286–300. DOI:10.1096/fj.201800062RR.
[67] Birghan C, Mundt E, Gorbalenya AE. A non-canonical lon proteinase lacking the ATPase domain employs the ser-Lys catalytic dyad to exercise broad control over the life cycle of a double-stranded RNA virus. EMBO J. 2000;19(1):114–123.
[68] Lejal N, Da Costa B, Huet J C, et al. Role of Ser-652 and Lys-692 in the protease activity of infectious bursal disease virus VP4 and identification of its substrate cleavage sites. J Gen Virol. 2000;81 (Pt 4):983–992. DOI:10.1099/0022-1317-81-4-983.
[69] Kung MH, Lin YS, Chang TH. Aichi virus 3C protease modulates LC3- and SQSTM1/p62-involved antiviral response. Theranostics. 2020;10(20):9200–9213.
[70] Mohamud Y, Qu J, Xue Y C, et al. CALCOCO2/NDP52 and SQSTM1/p62 differentially regulate coxsackievirus B3 propagation. Cell Death Differ. 2019;26(6):1062–1076. DOI:10.1038/s41418-018-0185-5.
[71] Wen W, Li X, Yin M, et al. Selective autophagy receptor SQSTM1/p62 inhibits Seneca Valley virus replication by targeting viral VP1 and VP3. Autophagy. 2021;17(11):3763–3775. DOI:10.1080/15548627.2021.1897223.
[72] Wu Y, Peng C, Xu L, et al. Proteome dynamics in primary target organ of infectious bursal disease virus. Proteomics. 2012;12 (11):1844–1859. DOI:10.1002/pmic.201100479.
[73] Zheng X, Hong L, Li Y, et al. In vitro expression and monoclonal antibody of RNA-dependent RNA polymerase for infectious bursal disease virus. DNA Cell Biol. 2006;25(11):646–653. DOI:10.1089/dna.2006.25.646.
[74] Wang Y, Wu X, Li H, et al. Antibody to VP4 protein is an indicator discriminating pathogenic and nonpathogenic IBDV infection. Mol Immunol. 2009;46(10):1964–1969. DOI:10.1016/j.molimm.2009.03.011.
[75] Deng T, Hu B, Wang X, et al. Inhibition of antiviral innate immunity by avibirnavirus VP3 via blocking TBK1-TRAF3 complex formation and IRF3 activation. mSystems. 2021;6(3):e00016–21. DOI:10.1128/mSystems.00016-21.
[76] Peng H, Yang F, Hu Q, et al. The ubiquitin-specific protease USP8 directly deubiquitinates SQSTM1/p62 to suppress its autophagic activity. Autophagy. 2020;16(4):698–708. DOI:10.1080/15548627.2019.1635381.
[77] He X, Chen G, Yang L, et al. Role of naturally occurring genome segment reassortment in the pathogenicity of IBDV field isolates in Three-Yellow chickens. Avian Pathol. 2016;45(2):178–186. DOI:10.1080/03079457.2016.1139687.